Report No. UT-17.21

BALANCED ASPHALT CONCRETE MIX PERFORMANCE

PHASE II: ANALYSIS OF BBR AND SCB-IFIT TESTS

Prepared For:

Utah Department of Transportation
Research Division

Submitted By:

University of Utah
Department of Civil and Environmental Engineering

Authored By:

Pedro Romero, Ph.D., P.E.
Kevin VanFrank, P.E.

Final Report
December 2017

RESEARCH
UDOT Keeping Utah Moving
Utah Department of Transportation - Research Division
4501 South 2700 West - P.O. Box 148410 - SLC,UT 84114-8410

DISCLAIMER

ACKNOWLEDGMENTS

The authors acknowledge the Utah Department of Transportation (UDOT) for funding this research, and the following individuals from UDOT on the Technical Advisory Committee for helping to guide the research:

- Scott Andrus
- Howard Anderson
- Steve Anderson
- Kevin Nichol

The authors also acknowledge the following individuals and their work. A significant portion of the information contained in this report is the result of their hard work. This includes the following current and former graduate students:

- Abu Sufian Mohammad Asib
- Faramarz Safazadeh
- Daniel Sudbury, M.Sc.
- Yang Li, M.Sc.

The following people also provided value input for this work:

- Tim Biel from PEPG (formerly CME)
- Michael VanMilligen, from PEPG (formerly CME)
- Clark Allen from Utah Department of Transportation

The authors also acknowledges the financial contribution from the Mountains Plains Consortium.

TECHNICAL REPORT ABSTRACT

1. Report No.
UT- 17.21

2. Government Accession No.
N/A

3. Recipient's Catalog No.
N/A

4. Title and Subtitle
Balanced Asphalt Concrete Mix Performance, Phase II: Analysis of BBR and SCB Tests

5. Report Date
December 2017

6. Performing Organization Code

7. Author(s)
Pedro Romero, Ph.D., P.E. and Kevin VanFrank, P.E.

8. Performing Organization Report No.

9. Performing Organization Name and Address
University of Utah
Department of Civil and Environmental Engineering
110 Central Campus Drive #2000
Salt Lake City, Utah Zip 84112

10. Work Unit No.
5H07803H

11. Contract or Grant No.
16-8427

12. Sponsoring Agency Name and Address
Utah Department of Transportation
4501 South 2700 West
P.O. Box 148410
Salt Lake City, UT 84114-8410

13. Type of Report & Period Covered
Final
Nov 2015 to Dec 2017

14. Sponsoring Agency Code
UT15.102

15. Supplementary Notes
Prepared in cooperation with the Utah Department of Transportation and the U.S. Department of Transportation, Federal Highway Administration

16. Abstract

An evaluation of the ability of the BBR and the IFIT tests to determine changes in asphalt mixture parameters was conducted as well as the possible implications of adoption these two tests at low and intermediate temperatures. It was found that the FI from the IFIT was a more sensitive parameter than the creep modulus or m-value from the BBR to detect changes in binder content; the reverse was true for air voids. Both tests indicate that RAP is detrimental to the overall expected performance of the mixtures when compared to a mixture with no RAP. However, the BBR appears to be a more sensitive test to capture the effect of aging and RAP on the material.

It was found that aging of the loose mixture at 135 °C prior to compaction shows a more consistent trend that aging the compacted specimen at 80 °C in both tests. One hour of loose mix aging at 135 °C results in the same mechanical changes as 47 to 55 hours of compacted mix aging at 80 °C.

Based on the results, it is concluded that adoption of the IFIT as a required test for mixture acceptance would likely result in mixtures with higher binder content being favored during design; no such changes would be expected with the adoption of the BBR as a required test. At the same time, the BBR appears to be a more sensitive test to capture the effect of aging and RAP on the material. Thus, adoption of the BBR as a specification test would likely result in changing the mixture design process to favor mixes with lower RAP content and less sensitivity to aging..

17. Key Words
Asphalt Concrete, Pavement Cracking, Bending Beam Rheometer, Flexibility Index, Recycled Asphalt Pavement.

18. Distribution Statement
Not restricted. Available through:
UDOT Research Division
4501 South 2700 West
P.O. Box 148410
Salt Lake City, UT 84114-8410
www.udot.utah.gov/go/research

23. Registrant's Seal
N/A

19. Security Classification (of this report)
Unclassified

20. Security Classification (of this page)
Unclassified

21. No. of Pages
86

22. Price
N/A

TABLE OF CONTENTS

LIST OF TABLES

LIST OF FIGURES

UNIT CONVERSION FACTORS

Units used in this report and not conforming to the UDOT standard unit of measurement (U.S. Customary system) are given below with their U.S. Customary equivalents:

- 25.4 millimeters (mm) = 1 inch (in)
- 1 megapascal (MPa) = 145.04 pounds per square inch (psi)
- 1 Newton (N) = 0.2248 pounds force (lbs)

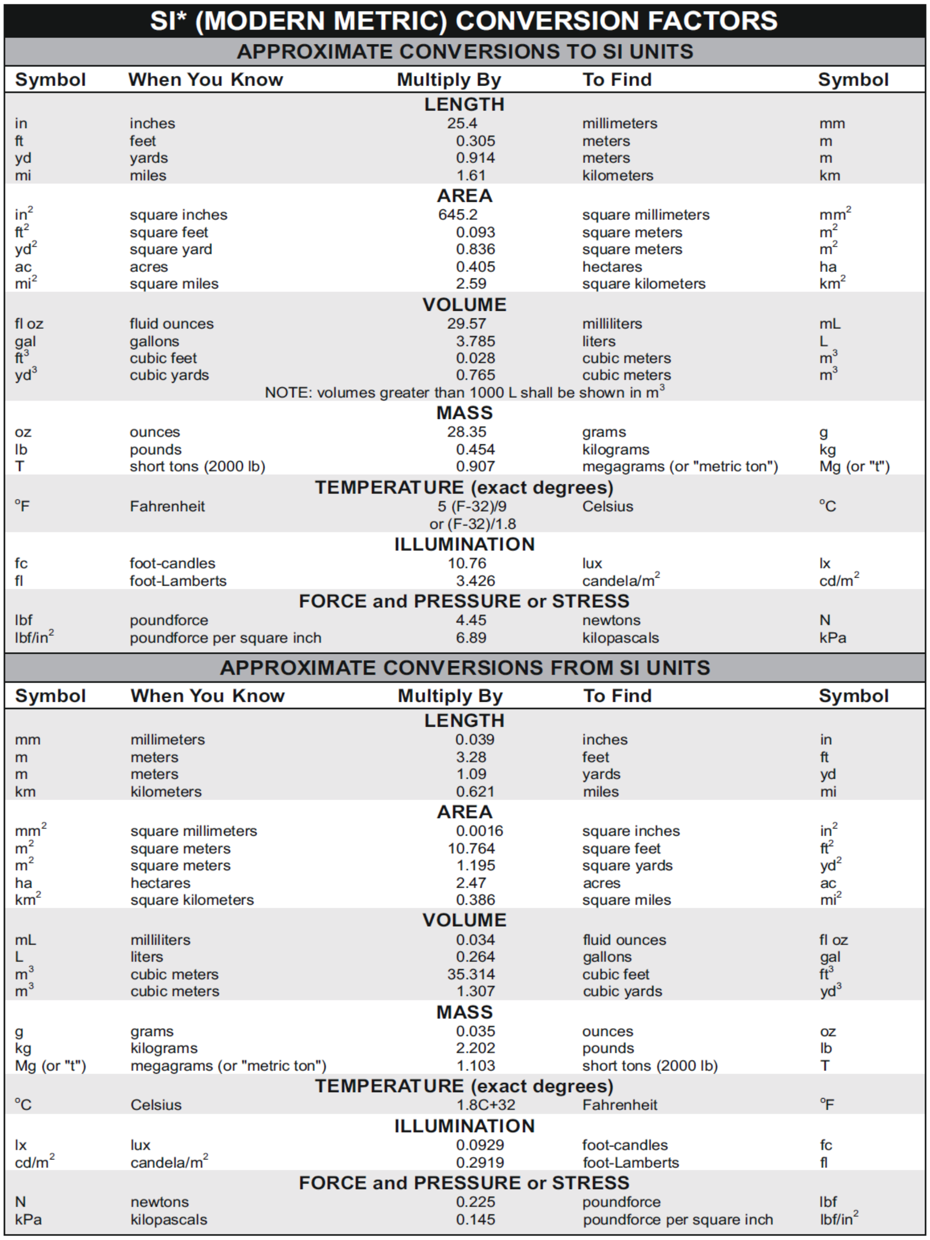

SI* (MODERN METRIC) CONVERSION FACTORS

APPROXIMATE CONVERSIONS TO SI UNITS

Symbol	When You Know	Multiply By	To Find	Symbol
		LENGTH		
in	inches	25.4	millimeters	mm
ft	feet	0.305	meters	m
yd	yards	0.914	meters	m
mi	miles	1.61	kilometers	km
		AREA		
in^2	square inches	645.2	square millimeters	mm^2
ft^2	square feet	0.093	square meters	m^2
yd^2	square yard	0.836	square meters	m^2
ac	acres	0.405	hectares	ha
mi^2	square miles	2.59	square kilometers	km^2
		VOLUME		
fl oz	fluid ounces	29.57	milliliters	mL
gal	gallons	3.785	liters	L
ft^3	cubic feet	0.028	cubic meters	m^3
yd^3	cubic yards	0.765	cubic meters	m^3
		NOTE: volumes greater than 1000 L shall be shown in m^3		
		MASS		
oz	ounces	28.35	grams	g
lb	pounds	0.454	kilograms	kg
T	short tons (2000 lb)	0.907	megagrams (or "metric ton")	Mg (or "t")
		TEMPERATURE (exact degrees)		
°F	Fahrenheit	5 (F-32)/9 or (F-32)/1.8	Celsius	°C
		ILLUMINATION		
fc	foot-candles	10.76	lux	lx
fl	foot-Lamberts	3.426	candela/m^2	cd/m^2
		FORCE and PRESSURE or STRESS		
lbf	poundforce	4.45	newtons	N
lbf/in^2	poundforce per square inch	6.89	kilopascals	kPa

APPROXIMATE CONVERSIONS FROM SI UNITS

Symbol	When You Know	Multiply By	To Find	Symbol
		LENGTH		
mm	millimeters	0.039	inches	in
m	meters	3.28	feet	ft
m	meters	1.09	yards	yd
km	kilometers	0.621	miles	mi
		AREA		
mm^2	square millimeters	0.0016	square inches	in^2
m^2	square meters	10.764	square feet	ft^2
m^2	square meters	1.195	square yards	yd^2
ha	hectares	2.47	acres	ac
km^2	square kilometers	0.386	square miles	mi^2
		VOLUME		
mL	milliliters	0.034	fluid ounces	fl oz
L	liters	0.264	gallons	gal
m^3	cubic meters	35.314	cubic feet	ft^3
m^3	cubic meters	1.307	cubic yards	yd^3
		MASS		
g	grams	0.035	ounces	oz
kg	kilograms	2.202	pounds	lb
Mg (or "t")	megagrams (or "metric ton")	1.103	short tons (2000 lb)	T
		TEMPERATURE (exact degrees)		
°C	Celsius	1.8C+32	Fahrenheit	°F
		ILLUMINATION		
lx	lux	0.0929	foot-candles	fc
cd/m^2	candela/m^2	0.2919	foot-Lamberts	fl
		FORCE and PRESSURE or STRESS		
N	newtons	0.225	poundforce	lbf
kPa	kilopascals	0.145	poundforce per square inch	lbf/in^2

*SI is the symbol for the International System of Units. (Adapted from FHWA report template, Revised March 2003)

LIST OF ACRONYMS

AASHTO	American Association of State Highway and Transportation Officials
BBR	Bending Beam Rheometer
CME	Construction Materials Engineering
CoV	Coefficient of Variation – Percent Ratio of the Standard Deviation to the Mean
FHWA	Federal Highway Administration
FI	Flexibility Index AASHTO TP-124
HWT	Hamburg Wheel Tracking Test, AASHTO T-3
IFIT	Illinois Flexibility Index Test, AASHTO TP-124
ITS	Indirect Tensile Strength, ASTM D6931
LSU	Louisiana State University
MEPDG	Mechanistic Empirical Pavement Design Guide
ME	Mechanistic Empirical
PG	Performance Grade, AASHTO M-320
RAP	Recycled Asphalt Pavement
SCB	Semi-Circular Bending Test
SGC	Superpave gyratory Compactor, AASHTO T-312
UDOT	Utah Department of Transportation
VFA	Voids Filled with Asphalt
VMA	Voids in the Mineral Aggregate
VTM	Voids in the total mix
VECD	Visco-elastic Continuum Damage

EXECUTIVE SUMMARY

A research project was conducted to determine the ability of the Bending Beam Rheometer (BBR) and the Semi-Circular Bend Flexibility Index (SCB-FI) to evaluate the effects of mix design factors such as binder content, air voids, RAP content, and laboratory aging on the predicted mixture performance at low and intermediate temperatures. The goal of this research was not only to understand the capability of each tests to relate to performance but also to evaluate what effect they will have on asphalt mixtures produced in the state. The experiment was separated into two parts, changes in binder content and air voids, and RAP content and aging.

In regards to the air voids and binder content, it was found that while the FI seems to be a more sensitive parameter than the creep modulus or m-value to changes in binder content; the reverse is true for air voids. A decrease in creep modulus was observed with increased air voids but only a step function was seen in the FI. While both tests show variations in results with changes in volumetrics (binder content and air voids), neither of these tests is expected to be used for volumetric verification as there are better tools available for this purpose.

In regards to the RAP content, both tests indicate that RAP is detrimental to the overall expected performance of the mixtures when compared to virgin mix. However, the data from the IFIT test indicates an asymptote as age increases and as RAP content increases while the data from the BBR shows no such trend. Based on this observations, the BBR appears to be a more sensitive test to capture the effect of aging and RAP on the material.

It was found that aging of the loose mixture at 135 ºC prior to compaction shows a more consistent trend that aging the compacted specimen at 80 ºC in both tests. An index valued developed as part of this study for the BBR results that combines both changes in modulus and changes in m-value. Using this index, equivalent times were obtained between both conditioning procedures. One hour of loose mix aging at 135 ºC results in the same mechanical changes as 47 to 55 hours of compacted mix aging at 80 ºC. The SCB IFIT test indicated that aging reduces the FI, with lower decrease seen at high binder contents.

Based on the results from both the low and intermediate temperature tests (the BBR and the IFIT), it was determined that increases in binder content are beneficial to the overall performance of the mixture (at least at low and intermediate temperatures). Deficiencies in binder content seem to be a problem for the BBR results as they indicate a desirable condition (lower modulus, same m-value), which is contrary to accepted knowledge. It is believed that adoption of the IFIT as a specification would likely result in mixtures with higher binder content being favored during design; no such changes would be expected with the adoption of the BBR.

The data from IFIT and BBR indicate aging causes mechanical changes in the material that relate to lower performance. The tests also indicate that RAP is detrimental to the overall expected performance of the mixtures when compared to virgin mixes. However, the data from the IFIT test indicates an asymptote as age increases and as RAP content increases while the data from the BBR shows no such limitation. Based on this observations, the BBR appears to be a more sensitive test to capture the effect of aging and RAP on the material. Thus, adoption of the BBR as a specification would likely result in changing the mixture design process to favor mixes with higher binder content with high RAP replacement.

The geometry of the SCB test seems to have a particularly high degree of effect on the FI results. While the geometry of the test lends particular importance to sample thickness notch thickness and notch depth; radius and thereby ligament length may play a minor role in the tail of the stress strain curve.

While more research is needed before the Flexibility Index is ready for adoption, it is recommended that the BBR modulus and m-value be used as parameters to evaluate low temperature properties of asphalt mixtures. Using these parameters, a true performance-based specification could be developed at the mix design stage.

1.0 INTRODUCTION

1.1 Problem Statement

An asphalt concrete pavement is ideally a continuous roadway having a smooth, unbroken surface while having the capacity to carry modern loading. Asphalt pavements are subject to distresses falling into five general categories. They are:

- Rutting- The permanent deformation of the pavement material from loads.
- Stripping – The separation of the binder from the aggregate.
- Fatigue Cracking – The development of cracks due to repetitive loads.
- Thermal Cracking – The development of cracks due to thermal contraction.
- Aging – The permanent change in the ability of the asphalt material to perform as designed, usually caused by oxidation or other chemical changes.

The design requirement that an asphalt pavement be continuous brings with it some challenging materials properties. One of the most interesting is the requirement that the pavement be able to expand and contract under temperature variation without breaking. This slow but repeated application of force will fracture even the strongest of materials; for example, a continuous steel rail track will break if curves are not provided allowing contraction to move the track transverse to the alignment while maintaining some continuity. An asphalt material is able to deal with these forces by its ability to relax stresses. So long as the stress relaxation is faster than the stress buildup, the material can relieve energy through flow and heat rather than the creation of new surfaces.

The ability of asphalt to relax stresses is reduced as the temperature decreases and as the rate of load application increases; therefore, testing of asphalt materials must consider both the temperature and the rate of load application. This requirement makes testing of asphalt materials more complicated in comparison to other construction materials. Since asphalt binder is the material that gives asphalt concrete its ability to relax stresses, many researchers have attempted to test the binder alone and link the behavior of asphalt binder to that of the asphalt concrete composite. However, this approach often fails to capture the interactions that occur between the asphalt binder and the aggregates, and more importantly, the effect of recycled asphalt pavement (RAP) and other additives. There has been only moderate success in this area and thus there is a need to develop practical tests of the asphalt concrete mixture (Mangiafico et al., 2016).

As the temperature increases and the speed of load application decreases, the behavior of asphalt materials changes and its ability to resist deformation decreases. This behavior leads to rutting. Over the past 30 years, many highway agencies, including UDOT, have given priority to rutting. UDOT has adopted the Hamburg Wheel Tracking (HWT) test to ensure sufficient rut resistance as well as to determine stripping susceptibility. Every mixture placed on Utah roads is tested for rut resistance at the design stage.

Emphasis on rutting behavior lead to the idea that rut-resistant mixtures, with high modulus could lead to thinner asphalt surfaces and cheaper pavements. (Hajj et al., 2005) However, actual field projects have shown that when highly stiffened asphalt concrete is used, cracking occurs, moisture enters the pavement structure, and the underlying layers weaken leading to premature pavement failure. An example of this behavior observed in 2012 on SR 201 and 3200 West ramp in Salt Lake City, UT is shown in Figure 1-1.

In response to the unbalanced mixture designs resulting from the emphasis on rutting, UDOT investigated the use of the Bending Beam Rheometer (BBR) in mixtures. Work done at the University of Utah and the University of Minnesota has shown that the BBR is a good alternative for asphalt mixture testing at low temperature (Zofka, et al., 2005, Ho and Romero, 2011, Romero, 2016).

The BBR places a constant load on a small asphalt mixture beam (12.5 x 6.75 x 127 mm (0.5 x 0.25 x 5 in)) and measures its deformation at mid-span; this process is described in detail in AASHTO TP125. The modulus of the material as well as the slope of the modulus vs time curve at 60 seconds have been successfully related to low temperature cracking performance (Jones et al, 2014, Romero, 2016). However, it is generally recognized that not all aspects of asphalt pavement performance can be addressed by measuring the modulus of the material. Some measurement of the strength or resistance to cracking of the material is also needed.

(a) Ramp facing north

(b) Close up of road showing cracks

(c) Ramp facing north-west

(d) Cracks on the road

Figure 1-1 Example of severely cracked road surface

Measuring the strength or resistance to cracking of a visco-elastic material such as asphalt concrete is difficult, not only due to the geometrical issues associated with tension tests, but also the previously mentioned effects of time and temperature. One approach that has been proposed is to load the material in cycles of tension and compression with a healing pause at the end of each cycle and the amplitude of the strain is incrementally increased until rupture occurs. The stiffness of the material is measured during each cycle. As the strain increases, force increases until damage begins to accumulate and the force required to produce the increment of strain then decreases. This effect is interpreted as damage. This complex method classifies material as to its resistance to strain induced damage and potentially allows the development of a model which measures the strain in a pavement structure under an assumed load, speed, and temperature. Each accumulated load/damage event is then added to reach the rupture of the pavement (Underwood et al, 2012). This is the Visco Elastic Continuum Damage (VECD) model and it is intended to be the future basis for crack prediction in the Mechanistic and Empirical Pavement Design Guide (MEPDG or ME guide). UDOT has attempted to perform the test envisioned for the VECD model and has found it to be difficult for a routine production setting.

An alternative approach, based on fracture mechanics concepts, was proposed by Mohammed at Louisiana State University (LSU) (Mohammad et al., 2012). This test uses semi-circular specimens fabricated from gyratory compactor samples and measures the energy required to propagate a crack. The test requires testing of several semi-circular specimens with pre-cut notches of three different lengths and measuring the area under the load-deformation curve at a constant temperature of 25 ºC (77F). The slope of the area versus the initial notch length is related to the fracture resistance of the mixture and its fatigue performance. This is described in ASTM D8044. VanFrank et al. (2017) evaluated this test for UDOT and concluded that it provided trends that were consistent with the expected behavior of the materials. However, the sample preparation, especially the different notch lengths, and the data analysis were deemed too difficult for routine testing. As a result, a simpler alternative was suggested.

Work performed at the University of Illinois has shown that the semi-circular bend (SCB) configuration, similar to the one proposed by LSU but using only one notch length, also relates to fatigue cracking performance. This test measures the area under the load-deformation curve and divides it by the slope of the unloading portion of the curve; this parameter is called the flexibility index (FI), and the test is called IFIT (Al-Qadi, et al., 2016). Having only one notch length reduces the number of specimens needed and simplifies the test, making it more attractive for everyday routine testing. Thus, it was determined that this test should be evaluated in Utah.

Given that UDOT has addressed the rutting and stripping behavior of its asphalt materials through the HWT tests, it is important to concentrate on the other distresses. The modulus and m-value at 60 seconds from the BBR and the FI from the IFIT have the potential to address thermal cracking and fatigue cracking, respectively. However, to allow for a better understanding of the optimum asphalt mixture properties, a conjoint evaluation of both tests is desirable. Such approach would lead to a balanced asphalt mixtures thus reducing premature failures and improving pavement performance.

1.2 Objectives

The objective of this research is to develop an understanding of asphalt mixture performance at low, intermediate, and high temperature and how the respective test, BBR, IFIT, and HWT, complement each other. Specific objectives are:

1. Determine how the introduction of low and intermediate temperature tests will affect the mixtures currently being used by UDOT in terms of binder content, RAP content, and aging.

2. Evaluate potential changes in mixture design resulting from the incorporation of low and intermediate temperature tests.

3. Optimize mixture parameters (binder content, RAP content) using low temperature tests (BBR) and intermediate temperature test (IFIT).

4. Verify the repeatability of the IFIT tests and the ability of both BBR and IFIT to detect changes in mixture components.

1.3 Scope

This study consists of the evaluation of asphalt mixture properties at two different temperature ranges (low and intermediate) using two different tests. One test, the BBR, addresses the cold temperature properties and the other, the SCB/IFIT, addresses the intermediate temperature properties of asphalt mixtures. Each test will explore the effects of increased or reduced binder content, increased RAP content, and increased laboratory aging on the same materials. Data will be produced by preparing samples appropriate to the BBR and the IFIT tests and testing them based on the respective protocols.

The results from this work will provide an understanding on how tests at low and intermediate temperature would potentially affect the mixtures that are placed in the state of

Utah. For this purpose, aggregates from local sources and a commonly used asphalt binder will be used in this study.

1.4 Outline of Report

This report is a continuation of the work previously described on the following research reports: *Development of Methods to Control Cold Temperature and Fatigue Cracking for Asphalt Mixtures* (Report No. UT-10-08) by Romero et al. (2011); *Using the Bending Beam Rheometer for Low Temperature Testing of Asphalt Mixtures* (Report No. UT-16.09) by Romero (2016); and *Intermediate Cracking in HMA: Phase I Semi-Circular Bending (SCB) Practicality Evaluation* (Report No. UT-17.01) by VanFrank, et al. (2017). While some information is repeated in this report for clarity and eased of reading, most of the theoretical background has been omitted as it has already been presented on those reports. Readers are encouraged to read the previous report available at the Utah Department of Transportation website: (www.udot.utah.gov/go/research).

This report is divided into the following chapters:

INTRODUCTION
TESTING OF ASPHALT MIXTURES
EFFECT OF BINDER CONTENT AND AIR VOIDS
    Bending Beam Rheometer
    SCB-IFIT
EFFECT OF RAP AND AGING
    Bending Beam Rheometer
    SCB-IFIT
SCB IFIT VARIABILITY
CONCLUSIONS
RECOMMENDATIONS AND IMPLEMENTATION
REFERENCES

2.0 TESTING OF ASPHALT MIXTURES

2.1 Overview

The performance requirements for asphalt pavements listed in Section 1.1 present a very interesting challenge in that asphalt mixtures must be evaluated based on mechanical tests that attempt to quantify those mechanical properties that are more relevant to the specific distress based on our understanding of material behavior. This is not always easy since there is the added requirement placed on test developers that whatever test is implemented will be somewhat practical for routine use. Furthermore, the mixtures used for evaluation must also represent the properties of materials that are placed on Utah roads. This section describes the testing of asphalt mixtures and the selection of materials to accomplish such a task.

2.2 Testing of Asphalt Mixtures

Testing of asphalt mixtures will be done using two tests, the BBR and the IFIT. These two tests have been previously evaluated by researchers and show promise in balancing the rigor with the practicality for determining mixture performance at low and intermediate temperatures. A short description of these tests is presented next.

2.2.1 Bending Beam Rheometer

The Bending Beam Rheometer, BBR, shown in Figure 2-1 and in Figure 2-2, produces the creep modulus and the stress relaxation capacity (slope of the modulus versus time curve in a log-log scale), also called m-value, by way of applying the elastic solution to a simply supported beam. These values obtained in asphalt binders have been used to evaluate low temperature performance in pavements (Bahia and Anderson, 1995; Marasteanu, 2004). Using the BBR to test asphalt mixtures in place of binder was originally proposed by Marasteanu et al. (2009) and further advanced by Ho (2010), Romero et al. (2011), Ho and Romero (2011), and Clendennen and Romero (2014) who determined that BBR testing of small amounts of material can produce behavioral results that are representative of the entire mixture.

Figure 2-1 Picture of Cannon Bending Beam Rheometer

Prior to testing, each sample is soaked in the temperature controlled bath for 60 minutes to ensure that the entire beam is brought to test temperature. Each test produces a series of data that includes force and deflection as a function of time. These values are then used to calculate creep modulus and the m-value (slope).

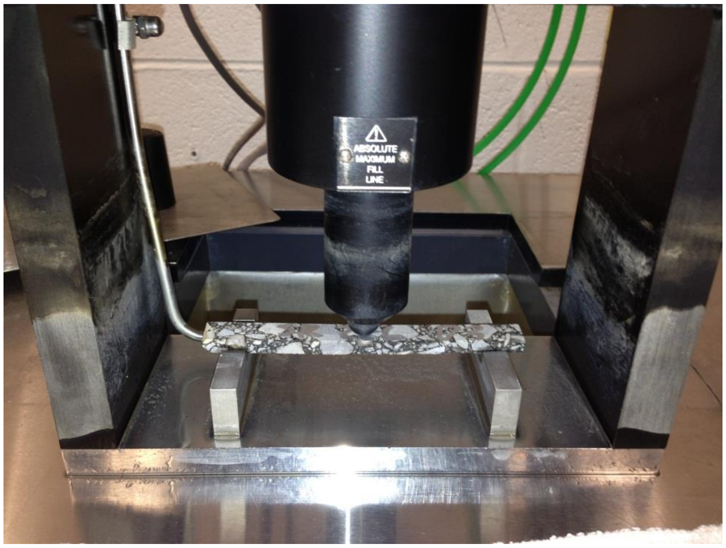

Figure 2-2 Sample beam in the BBR testing position (pictured out of bath for clarity)

2.2.1.1 Data Analysis

The BBR automatically records the load and the deformation of the beam. Knowing the beam dimensions and using beam elastic solutions along with elastic-viscoelastic correspondence principle, the creep modulus as a function of time of the material is determined. Standard software provided with the BBR automatically calculates the creep modulus and m-value at the end of the test and highlights these values at 60-seconds. Therefore, even though other times can be used, due to software convenience and consistency with binder testing, creep modulus and m-value at this specific loading time have been used to evaluate expected mixture performance.

More specific details of the BBR testing can be found in AASHTO Temporary Procedure TP 125-16: Standard Method of Test for Determining the Flexural Creep Stiffness of Asphalt Mixtures Using the Bending Beam Rheometer. The procedure is available at the AASHTO website.

2.2.2 Semi-Circular Bend Tests

During the 1990s, a test called Semi-Circular Bending Beam Test (SCB) was proposed to determine the crack resistance and crack growth rate of bituminous mixtures. It was believed that this configuration was easier in comparison to other methods that were expensive, complex, time-consuming for regular use, and difficult to perform (Krans et al., 1996). The SCB test gained some popularity for asphalt mixture fracture property characterization at low temperatures in the early 2000s and has since become a popular way to determine fracture toughness of HMA. Part of this is due to its simplicity in terms of specimen preparation using the SGC or coring from the field and testing method (*Hofman, et al., 2003, Molenaar, et al., 2002*). Many researchers studied fracture properties of asphalt specimen at low temperature to differentiate cracking resistance (Marasteanu et al., 2007; 2012; Arabani and Ferdowsi, 2009; Zofka and Brahman, 2009; Wang et al., 2016; Huang et al., 2005, 2019). Researchers worldwide established standard protocols to unify different methods of SCB test at low temperatures such as EN12697-44: 2010 and AASHTO TP105-2013. More recently, many researchers have studied and investigated the intermediate temperature fracture resistance of various asphalt mixtures using the same SCB test (Mull et al., 2006; Mohammad et al., 2004, 2012; Huang et al., 2013; Al-Qadi et al., 2015; and Nsengiyumy et al., 2015). The goal of all of these studies is to eliminate mixtures that have a tendency for premature failure through a cracking related mechanism by characterizing the fracture and fatigue resistance properties of the designed mixture in the laboratory prior to installation. However, special care has to be taken in producing the initial notch because the geometry and the quality of the notch tip may significantly affect the fracture behaviors of SCB specimens. Standard protocols have been developed for different methods such as ASTM D8044-2016 and AASHTO TP124-2016 to determine test procedures such as loading rate, specimen geometry, and support conditions, to obtain a value for the fatigue resistance.

Arabani and Ferdowsi (2009) studied SCB tests and compared them to a suite of conventional tests like the Indirect Tensile Strength, (ITS) to describe tensile strength, fracture, and fatigue properties of asphalt mixtures. It was observed that the SCB specimens fail with less distortion and a clear and anticipated crack path. The way in which SCB specimens fail indicates that tension must be the dominant failure mode even at intermediate temperatures. ITS test shows more of a wedging-type failure which indicates that a significant amount of energy from the specimen' s failure is due to the flow of materials or a mixed mode of stress conditions (Arabani and Ferdowsi, 2009).

Mull et al. (2002) investigated the applicability of the SCB specimen by J_c characterization. J_c is determined by using Equation 2-1:

$$\mathbf{J_c = -\left(\frac{1}{b}\right) \int \frac{dU}{da}} \qquad \textbf{Equation 2-1}$$

Where J_c = critical strain energy release rate (kJ/m^2), b = sample thickness (m), a = notch depth (m), and U = strain energy to failure (N.m). The utilization of the semi-circular specimen to determine the critical value of the J -integral intended to use at least two notch depths which is expressed in Equation 2-2:

$$\mathbf{J_c = \left(\frac{U_1}{b_1} - \frac{U_2}{b_2}\right) \frac{1}{a_2 - a_1}} \qquad \textbf{Equation 2-2}$$

This fracture resistance ranking, based on the J-integral values, seemed to be a promising tool in fatigue crack growth of asphalt mixtures. Monotonic loading SCB fracture tests measure either toughness or the critical strain energy release rate during a single displacement controlled loading until failure. To determine J_c, The area under the load-deformation curves at pre-peak regions is calculated to represent the strain energy value to failure (U) of specimens for each notch depth. The average values of U (calculated from replicate results) are then plotted against the different notch depths to compute a slope of a linear regression line, which is dU/da in the equation 2-1. The steeper the absolute value of the slope, the higher the J_c value and the tougher the material. The critical value of fracture resistance, J_c, is then computed by dividing the dU/da value with the width, b, of specimens. Mull et al. (2006) developed hysteresis loops to obtain energy release rate. It was observed that compliance of the specimen increases with increased crack length and area above the unloading curve obtained from hysteresis loops becomes larger. The increased area is representative of the increased energy expended on damage formation.

Following the concept of J_c, Mohammad et al. (2004, 2012) investigated the sensitivity of J-integral values with varied notch depths and different asphalt mixtures to the indirect tensile stress and strain test results. Their study asserted that the concept of toughness (fracture toughness) is directly related to intermediate temperature crack performance (fracture resistance) in pavements. The Louisiana State University Model (LSU) for crack propagation assumes that the energy (toughness) to move a crack at any point along the developing crack path is the energy under the stress-strain curve until the strain achieved at the load that begins the crack propagation. They observed that J-integral values from the semi-circular fracture test were fairly sensitive to the change in asphalt binder type. It was found that the SCB measured J_c values demonstrated a good correlation with field cracking performance data.

Al-Qadi et al. (2015) presented a test method that to calculate fracture energy and the flexibility index known as IFIT testing method. In contrasts to previous work, this method only uses one notch length. They found that the results have consistent and repeatable trends that corresponded to changes in AC mixture design properties. The Flexibility Index is calculated using Equation 2-3:

$$FI = A \times \frac{\mathbf{Gf}}{\mathbf{abs(m)}}$$ **Equation 2-3**

Where G_f is work of fracture obtained by finding the area under the load-displacement curve and dividing by the crack propagation area reported in joules/m^2 and m is slope of the post-peak curve at the inflection point reported as kN/mm. Coefficient A is a unit conversion factor and scaling coefficient.

Nsengiyumva et al (2015) investigated an experimental-statistical approach on SCB testing variables (i.e., the minimum recommended number of specimens, thickness, notch length, loading rate, and testing temperature) to evaluate fracture behavior of AC mixtures at intermediate service temperature conditions. Based on the test-analysis outcomes, they came to the conclusion that a temperature of 21˚C, loading rate of 0.1 to 0.5 mm/min, 5 mm length of the notch, thickness of 40 to 60 mm and a minimum of five to six samples are the statistical specifications to sufficiently represent fracture behavior of asphalt samples.

2.2.2.1 SCB IFIT Sample Preparation and Testing Procedures

For this work, testing is done in accordance with AASHTO TP124-16 on samples built from a 160-mm tall, 150 ± 1-mm diameter gyratory pucks made from mixture designs discussed in Section 2.3. Since the same asphalt binder was used for the two mixes, mixing temperature was 320°F and compaction was done at 305°F. Mixes were aged for two hours in an electric, convection oven at the mixing temperature prior to compaction. Compaction was done to height to obtain the target air voids. The volume of the mold at 160-mm was calculated in cubic centimeters, multiplied by the theoretical maximum specific gravity and then by 0.910. An adjustment of 1.5% was used to compensate for the void distribution in the compacted sample. Minor adjustments were made to this factor as densities were verified. Upon loading the gyratory mold, a thin spatula was inserted 6 times around the edge of the mold and to the depth of the mold to reduce the rock texture at the sample surface. Three replicate gyratory pucks were produced for each test condition.

On the day following compaction, two, 60±1-mm thick disks were cut from the center of each 160 mm compacted puck. Bulk specific gravities were measured on the two disks to assure they met the 92.5 ± 0.5% target density. Dryback was done in an Instrotek CoreDry® device prior to the dry weight measurement. The disks were then cut across the diameter to make half circles. A 15±1-mm deep notch was then cut across the center of the flat side. All cuts were done with saws and templates manufactured by TestQuip for this purpose and shown in Figure 2-3. All dimensions were measured with a micrometer to 0.1-mm and recorded for use in the calculations. All four of these notched, half rounds were then dried and incubated in conditioned air to 25 ± 0.5°C in preparation for testing. Tests were run at a displacement rate of 50-mm per minute as specified in AASHTO TP124. All tests were performed in open air on a Test-Quip load frame built specifically for IFIT testing and shown on Figure 2-4. Data was collected electronically and then processed using the Test-Quip QT-34 software.

Figure 2-3 TestQuip Saws

The TestQuip test frame is a servo-hydraulic system using paired (averaged) line-load displacement control and measurement. Displacement measurement is done at 40 hz. This frequency equates to 2.89-$\mu\epsilon$ per measuring increment assuming a 1.5-mm notch width and a 15-mm notch depth. The frame rollers are suspended on bearings and there is no contact between the actuator and the roller allowing for a low friction actuator travel. The data trace is of excellent quality requiring little, if any, model fitting. An accurate integral can generally be obtained directly from the data using the trapezoidal rule. The QT-34 data analysis software was tested against the Illinois IFIT analysis software (https://apps.ict.illinois.edu/software/) using data produced on the TestQuip load frame with good agreement in Flexibility Index values.

Figure 2-4 TestQuip Test Frame with Test Head

2.3 Selection of Asphalt Mixtures

In order to evaluate how both the BBR and the IFIT might affect the mixture designs, the same materials were used to perform all testing. Two different virgin mixture designs that met the Superpave requirements were obtained from local contractors. One of these mixes, referred to as Mix A, is a 19-mm nominal maximum aggregate size (NMAS), 100 gyration Ndes, while the other, referred to as Mix B is a 12.5-mm NMAS, 75 gyration Ndes. A single asphalt binder graded as PG 64-28-UT was also selected to represent typical material used in the state and a local source of RAP was obtained and used for all mixture variants. RAP binder content was approximately 5.2% by mass of the RAP with minor variation in the stockpile. The collected quarry aggregate was separated into individual sieve sizes. Sieve size #200 was washed to control the amount of dust filler entering into the mix. One percent hydrated lime based on the virgin aggregate weight was added in a 3:1 slurry to all mixes. The gradations of mixes A and B are shown on Figure 2.5. Mix A is made with a low absorption limestone and Mix B is made with a mixture of quartzite and granite. Tests done using the Hamburg Wheel Tracking (HWT) during mixture design indicated both of the virgin mixes to be rutting and stripping resistant with HWT tests exhibiting less than 5-mm of rut depth and no secondary deformation slope in 20,000 passes at 50°C.

As part of the air voids and binder content investigation, a variant of Mix A had to be used in the BBR testing. The adjustment in gradation came from not meeting volumetric properties set by AASHTO R35 Superpave specifications as both the number of gyrations used for compaction and the binder content were varied. The amount passing the coarse aggregate sieves was increased while the percent passing the fine aggregates sieves was decreased to create more of an “S” shape curve and support the changes. However, due to the fact that each combination either received different compaction effort or binder content, it was not practical to meet AASHTO R35 specifications for each sample. The actual details of the mixture variants are discussed in in Section 3.2 of this report.

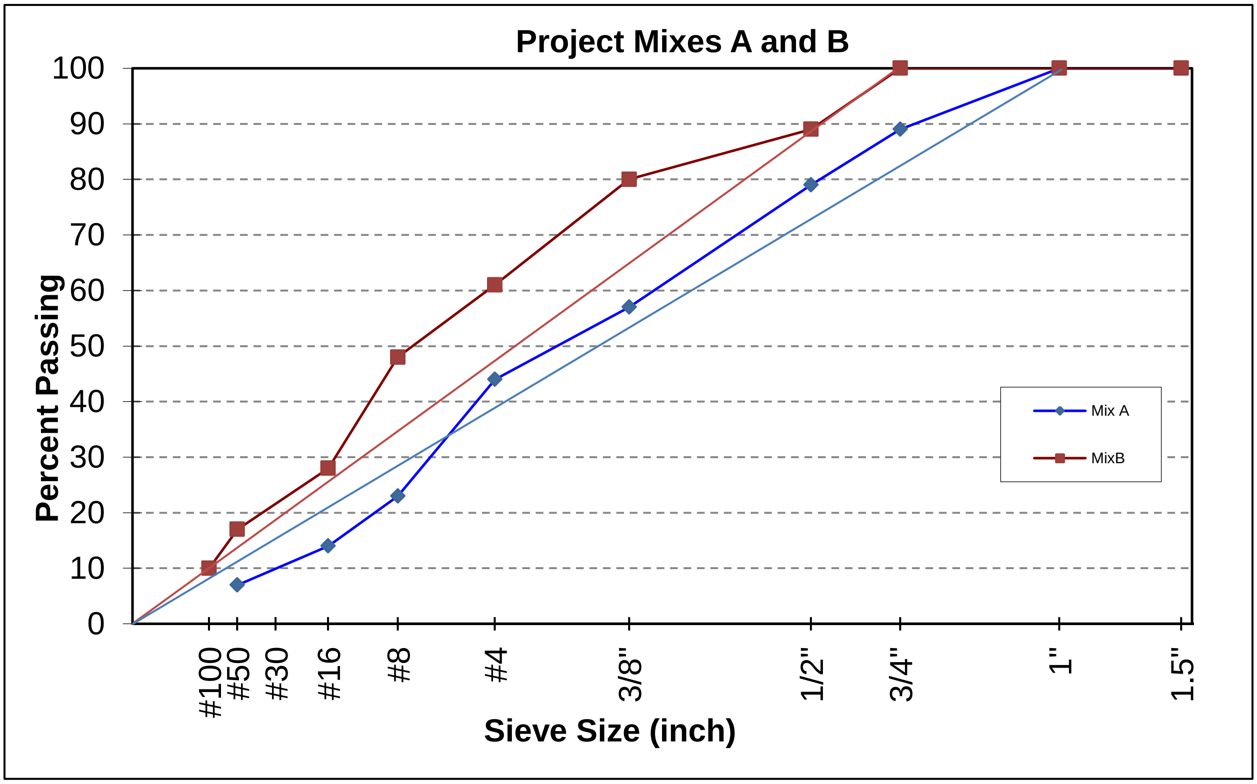

Figure 2-5 Base Mixture Gradations

2.4 Summary

This chapter presents a background of the testing procedures used to characterize the low and intermediate temperature of asphalt mixtures. A short description of the BBR was given; however, a more detailed description can be found on previous UDOT reports as listed in Section

1.4 of this report. A literature review of the SCB tests is provided, followed by a description of the procedures used in this study.

Given the effect that these tests might have on future mixture design, the same two asphalt mixtures and one local asphalt binder was used in both the BBR and the IFIT tests as described in Section 2.3. This was needed to allow for direct comparisons between the results of both tests. However, it should be understood that BBR and SCB IFIT tests are at different stages of development. As previous UDOT reports have presented, the variability and reproducibility of the BBR test are well understood. However, the SCB IFIT test still needs further development. This difference should be considered when evaluating the results. Some observations regarding the variability of the IFIT tests are discussed in Section 5.0.

3.0 EFFECT OF BINDER CONTENT AND AIR VOIDS

3.1 Overview

The binder content and the air voids of an asphalt mixture are two variables that are known to affect the mechanical behavior of the materials. It is important, therefore, to evaluate the ability of any test to capture the effects of both binder content and air voids. Alternatively, it is desirable to know the tolerances regarding these two variables when performing any test or if the tolerances, as proposed, yield accurate results.

An experiment was set up in which both the binder content and the air voids were varied. Ideally, those two factors are isolated; however, varying one will affect the other so both binder content and air voids were evaluated simultaneously. The results for both tests are discussed in this section.

3.2 Bending Beam Rheometer

The experimental design for the BBR consisted of two experiments: varying compaction level while keeping binder content constant and varying binder content while keeping compaction level constant. For each variation, Superpave gyratory compacted (SGC) cylinders were prepared at the University of Utah. The cylinders were cut into beams for testing on the BBR using the procedures outlined in AASHTO TP125.

After cutting, the beams were placed in a sealed container and tested after 24 hours. This was done to eliminate any variation that might be caused by steric hardening. Because the measured air voids of the SGC cylinders are not applicable to each individual cut beam, an alternative method had to be developed. Due to the size of the beams (6.25x12.5x101 mm, ~25 g) and typical asphalt absorption of 0.5%, it was not possible to perform the AASHTO T166 bulk density test with the available analytical balance. Instead, the density of each beam was estimated by dividing the mass over the volume of the prismatic beams. The volume was measured using calipers accurate to 0.02 mm and the mass using a balance sensitive to 0.01 g.

This density was compared to the theoretical maximum density determined according to AASHTO T209. These density values were used to calculate air voids where appropriate.

After labeling and volumetric measurements, 12 random samples were selected and evaluated for any possible damage, excessive air voids, or compaction that could likely affect test results. The two most excessively damaged samples were then removed from the sample population and the flexural creep modulus of the remaining beams was measured on the BBR. Each beam was conditioned in the BBR bath at the low temperature of -18 °C (PG+10°C) for 60 minutes prior to testing. The creep modulus as well as the m-value at 60 and 120 seconds were recorded and used for analysis. Based on the time temperature superposition principle, this is equivalent to testing the same binder at two different temperatures or testing two binders of different grades at the same temperature.

3.2.1 Mixture Properties

As was discussed in Section 2.3, two variations of Mix A were used in this experiment. The gradation is almost the same as that shown in Figure 2-5; however, due to the changes in both binder content and air voids, each sample had slightly different volumetric properties. These volumetric properties are shown in Table 3-1 and Table 3-2.

Table 3-1 Volumetric Properties of Samples for the Air Void Experiment

Mix A Variant I						
Binder Content, %	**Pb**	4.2				
Binder Grade	**PG**	64-28				
Design Gyrations	**N_{des}**	70	60	60	40	30
Air Voids, %	**VTM**	2.3	4.5	4.5	5.4	6.2
VMA, %	**VMA**	11.55	13.62	13.62	14.42	15.07
VFA, %	**VFA**	80.08	66.96	66.96	62.55	58.87
Dust Proportion	**D/B**	1.3				
Bulk SG	**G_{mb}**	2.432	2.375	2.375	2.353	2.225
Max. SG	**G_{mm}**	2.488				

Table 3-2 Volumetric Properties for the Binder Content Experiment

Mix A Variant II							
Binder Content, %	**Pb**	5.0	5.5	4.7	4.4	4.1	3.8
Binder Grade	**PG**	64-28					
Design Gyrations	**N_{des}**	75					
Air Voids, %	**VTM**	0.6	0.5	1.7	3.4	3.9	6.4
VMA, %	**VMA**	12.93	13.11	12.80	13.36	13.16	14.38
VFA, %	**VFA**	95.36	96.18	86.72	74.55	70.36	55.49
Dust Proportion	**D/B**	1.10	1.07	1.20	1.30	1.40	1.60
Bulk SG	**G_{mb}**	2.416	2.424	2.412	2.389	2.387	2.346
Max. SG	**G_{mm}**	2.431	2.436	2.453	2.472	2.483	2.507

3.2.2 Air Voids

In this experiment compaction level varied while binder content was held constant (at optimum) as shown in Table 3-1. Optimum binder content on the variant mixtures was found to be 4.2% after a “sweep” was performed. Five SGC cylinders were compacted ranging from 30-70 gyrations at increments of 10 gyrations for each cylinder. The bulk density of each cylinder was measured using AASHTO T166 and compared to the theoretical maximum density of 2.488 for the mixture design according to AASHTO T209. The measured cylinder air voids ranged from 2.3% - 6.2% as is shown in Table 3-3.

The cylinders were then cut into bricks which were further reduced to beams for testing on the BBR as described in AASHTO TP125. As previously mentioned, for each SGC sample, 12 beams were randomly selected and the mean estimated air voids was measured. Air void measurements in Table 3-3 show that the difference in air voids between beams and cylinders is about 0.5%. This is within typical ranges observed in prior research (Romero et al 2011) and is believed to be the result of the smooth faces.

Table 3-3 SGC Cylinder's Air Voids and Mean Estimated Air Voids in Beams

Gyrations	Compacted Height, mm*	G_{mb}	Air Voids, %	
			Measured Cylinder	Estimated Beam
70	110.7	2.432	2.3	2.1
60	114.3	2.375	4.5	5.1
50	114.2	2.375	4.5	6.0
40	115.5	2.353	5.4	6.0
30	116.3	2.335	6.2	6.8

*All samples had approximately the same mass

3.2.2.1 Air Void Results

Figure 3-1 shows that creep modulus increases with increasing compaction effort. It is believed that the space from the increased air voids at lower compaction levels allows for greater movement and thus results in a lower creep modulus. Figure 3-2 shows that there is a general trend of decreasing modulus with increasing air voids at both 60 & 120 seconds. In contrast, the 60 and 120 second m-value for beams in Figure 3-3 seem to show no discernable trend in m-value with increasing air voids.

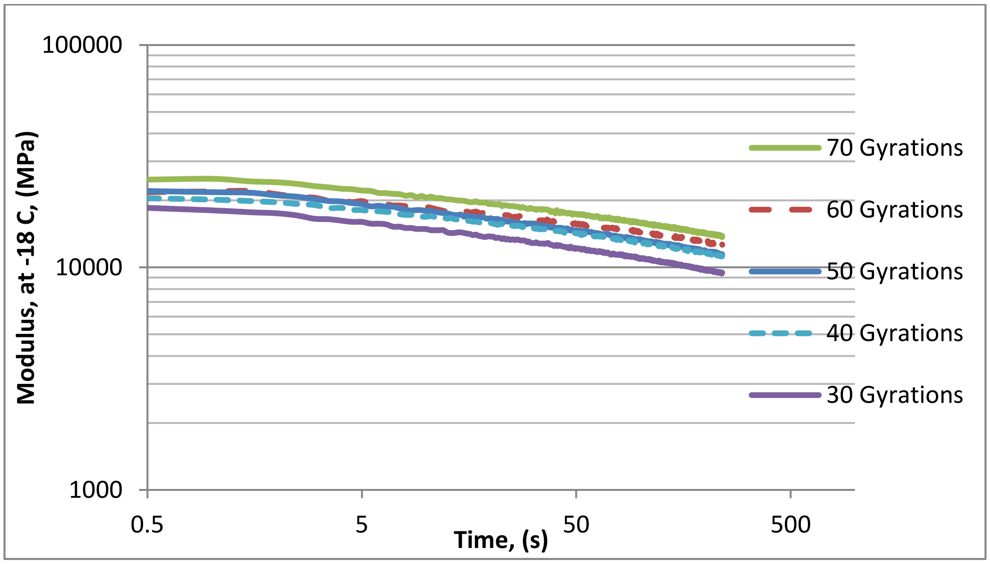

Figure 3-1 Average BBR results for varying compaction effort, binder content constant.

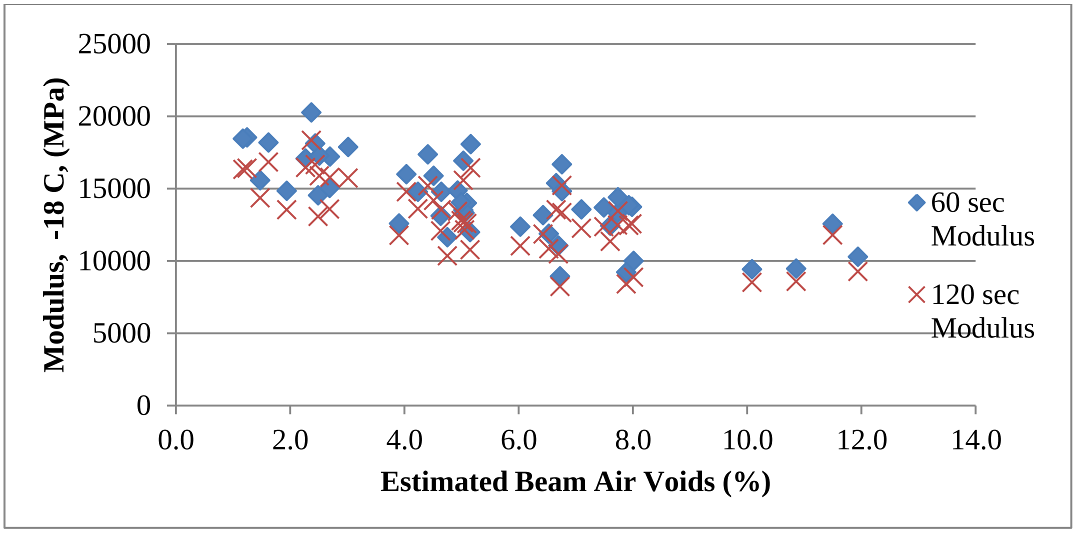

Figure 3-2 Beam stiffness with varying compaction effort, binder content constant.

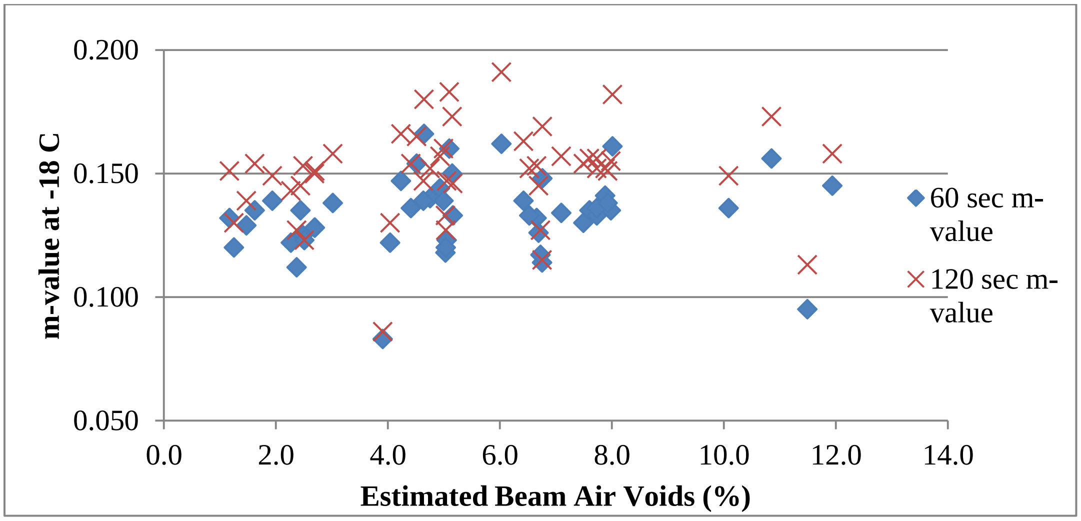

Figure 3-3 Beam m-value at varying compaction effort, binder content constant.

To aid in the analysis and reduce some of the noise, the air voids were separated into discrete groups of 2 percent increments. This is shown in Figures 3-4 and 3-5. It is evident that the creep modulus decreases as the air voids increase. However, the same is not observed in the m-value as there is no discernable trend.

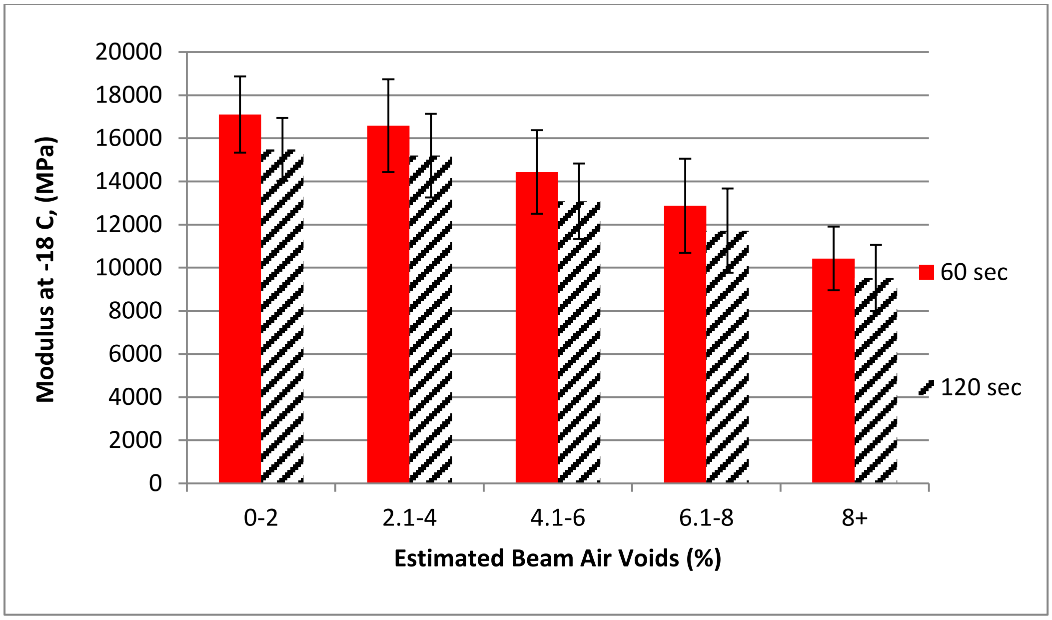

Figure 3-4 Average stiffness per air void grouping, binder content constant.
Error bar represents 1 S.D.

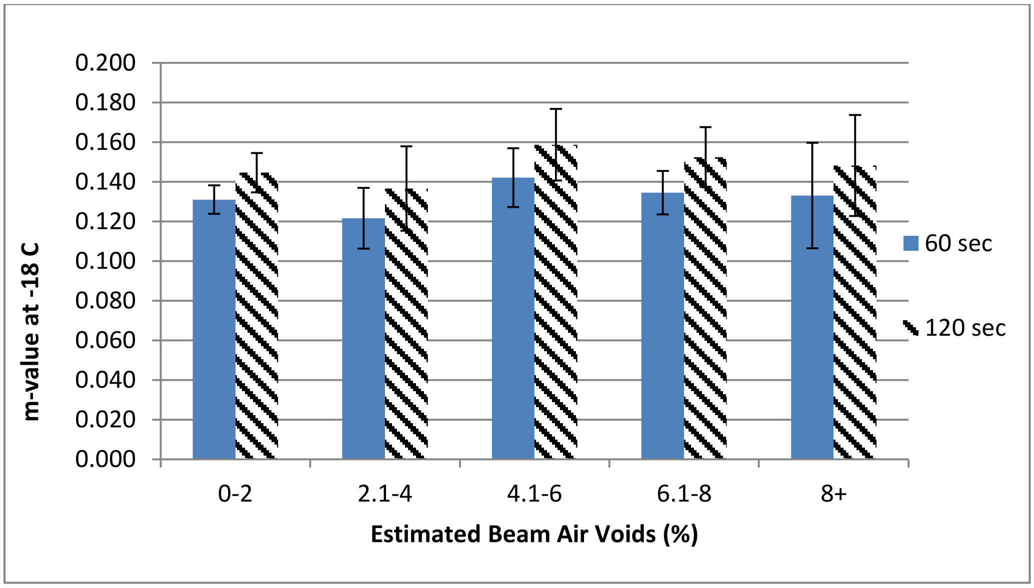

Figure 3-5 Average m-value per air void grouping, binder content constant.
Error bars represents 1 S.D.

3.2.3 Binder Content

In this part of the experiment, the binder content was changed while the number of gyrations remained constant at 75. This resulted in compacted specimens with different properties as shown in Table 3-4. A binder sweep of the mixture was performed as was shown in Table 3-2. In the binder content experiment the cylinders used to determine the optimum binder content were the same samples that were used for the binder sweep. Binder content varied from 3.8% - 5.5% and air voids ranged from 0.5%-6.4%.

Table 3-4 SGC Cylinder's Air Voids and Estimated Air Voids in Beams, Varying Binder Content

Binder Content, %	Gyrations	Compacted Height, mm	G_{mb}	G_{mm}	Air Voids, %	
					Measured Cylinder	Mean Estimated Beam
5.0	75	112.4	2.416	2.430	0.6	0.0
5.5	75	111.8	2.424	2.436	0.5	2.9
4.7	75	111.6	2.412	2.453	1.7	1.6
4.4	75	113.8	2.389	2.472	3.4	4.5
4.1	75	112.9	2.387	2.483	3.9	3.0
3.8	75	115.7	2.346	2.507	6.4	7.7

*Mass of aggregate was the same but total mass varied according to binder content.

3.2.3.1 Binder Content Results

In the binder content experiment, with optimum binder at 4.2%, creep modulus values were highest for values closer to optimum. Figure 3-6 shows that the 4.1% binder content had the highest modulus followed by 4.4%. Creep modulus decreased with both increasing and decreasing binder content (from optimum). With increasing asphalt content, more asphalt is available to "flow" while decreasing asphalt content results in more voids and thus increased deflection as discussed in Section 3.2.1. Figure 3-7a shows changes in creep modulus with air voids for different binder contents. The lowest binder content of 3.8% shows a greater spread of air voids. This is most likely because the binder distribution in the beams was uneven as there was an overall deficiency in binder content. The 120-second measurements in Figure 3-8a show similar results.

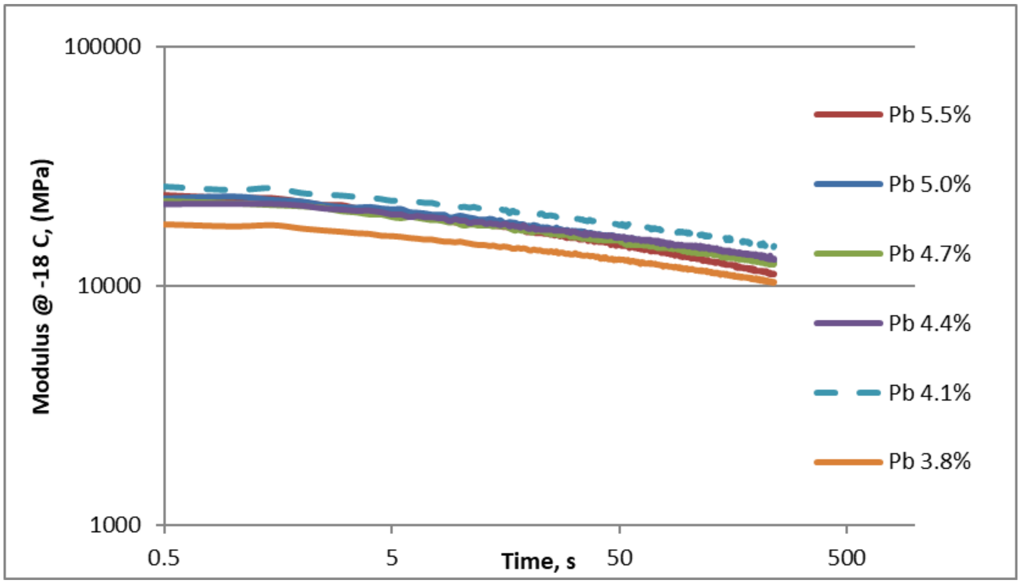

Figure 3-6 BBR creep modulus for varying binder content, compaction constant.

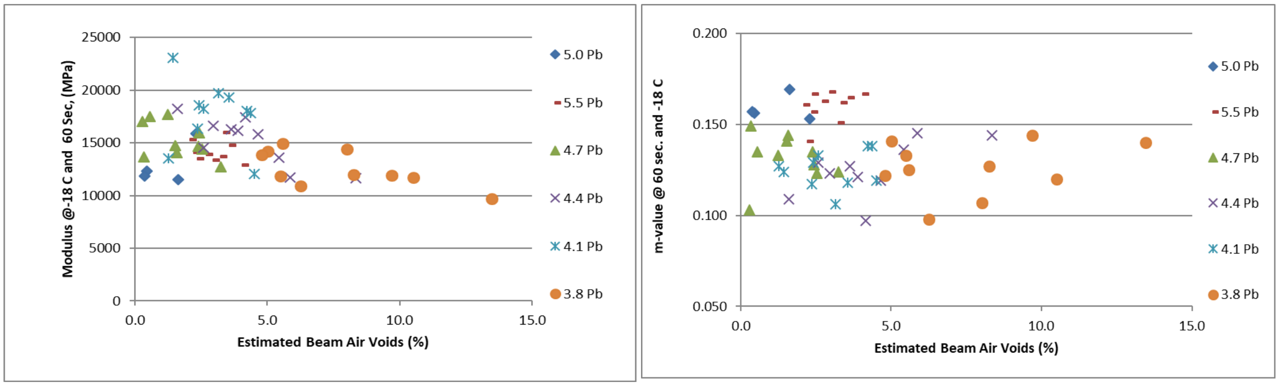

Figure 3-7 a. Creep modulus and b. m-value at 60 sec. varying binder contents, compaction constant.

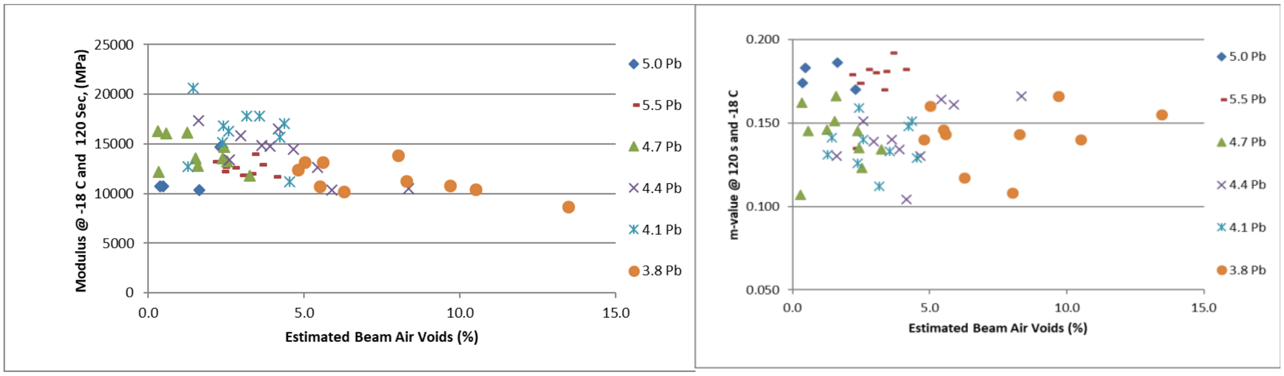

Figure 3-8 a. Creep modulus and b. m-value at 120 sec. varying binder content, compaction constant

Similarly to what was done with the air voids experiment, the data was separated into discrete values of air voids that resulted from the changes in binder content. Figure 3-9a shows that there is a trend of decreasing creep modulus with decreasing air voids groups. In contrast, evaluation of the m-value in Figure 3-9b for air void grouping shows that negligible change occurs at different air void contents and no clear pattern is observed.

Figure 3-10 shows the average values for different binder contents. For binder content above the optimum (4.2% for gradation and compaction), only a small decrease in creep modulus is observed. A small decrease in binder content below optimum (4.1%) shows a noticeable increase in creep modulus; further reduction in binder content to 3.8% reverses the trend showing an actual decrease in modulus. This is similar to what is observed in Figure 3-6. The reason for this behavior is believed to be changes in film thickness and how it changes the ability of the aggregates to move in relation to one another; however, at some point, there is a loss of cohesion resulting in a lower modulus. Thus, the amount of asphalt binder available plays a significant role in the creep modulus of binder deficient mixtures but not so much in mixtures with excess binder. It is not known if this behavior applies to different gradations or if it is specific to the mixture used in this portion of the study. Analysis of the m-value shows only slight variations as the binder content changes. The m-value is related to the relaxation capacity of the material and this property does not change with air voids or film thickness.

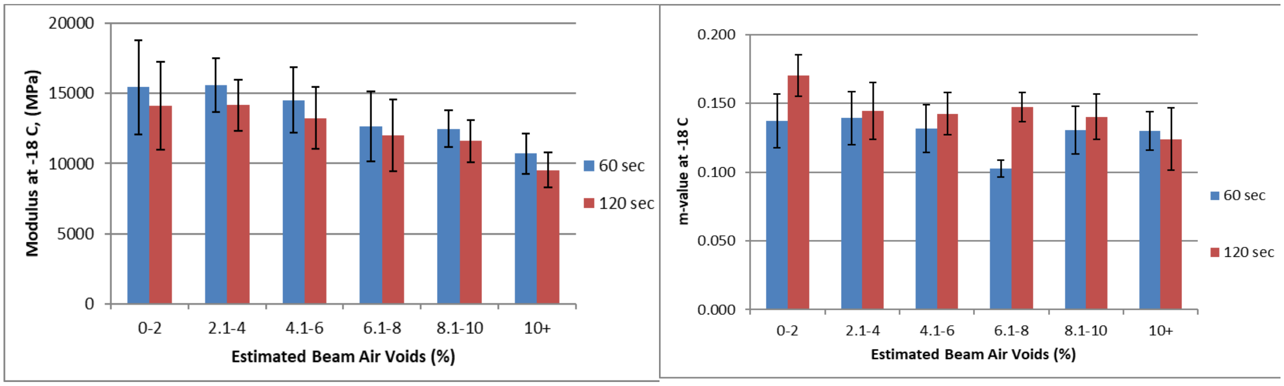

Figure 3-9 a. Average creep modulus and b. average m-value per air void grouping at 60 and 120 sec., binder content varied.

Error bars represent 1 S.D.

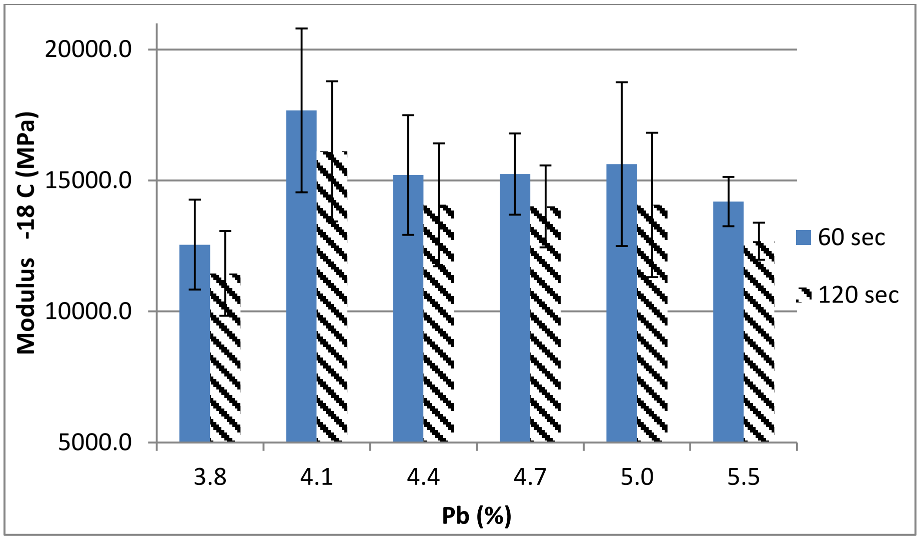

Figure 3-10 Average creep modulus per binder content grouping, compaction constant

Error bars represent 1 S.D.

3.3 SCB IFIT

Similarly to the case of low temperature performance, understanding the effects of binder content and air voids in a mixture may be important to control the fatigue cracking behavior of pavements. It is believed that variations in these properties have significant effects in the performance of asphalt mixtures once placed in the field. Also of importance is an understanding of the effect of these variables on test results so that the values are repeatable and reproducible. An experimental matrix was developed to investigate these variants.

3.3.1 Experimental Procedure

The IFIT testing was done as described in Section 2.2.2.1. To evaluate the between- lab repeatability, a set of samples were prepared and compacted in UDOT's laboratory and a separate set in CME's laboratory. All cuts, specific gravity measurements, incubation, and breaks were done on a single set of equipment in UDOT's laboratory but with different technicians; thus differences would be the result of sample preparation or equipment operator, not the machine itself.

Three replicate samples consisting of four test billets each were prepared at a target of 7 ± 0.5% voids based on AASHTO TP-124. For all combinations shown in to these mixtures; this allows for direct evaluation of the effect of binder content.

Table 3-5 shows the binder content used. Short term (2 hour) aging was done prior to compaction and no RAP was introduced to these mixtures; this allows for direct evaluation of the effect of binder content.

Table 3-5 SCB IFIT Binder Sweep Experimental Matrix

	Binder Content		
Mix A	4.1%	4.6%	5.1%
Mix B	4.75%	5.25%	5.75%

3.3.2 Results and Analysis

It is known that in fracture testing, small samples will break at higher stresses than large samples (e.g., the lab sample breaks at a higher stress than the pavement). For this reason, all four billets were tested and the highest break result was discarded. The remaining three are averaged and presented as one data point. Three conditions of these average values, representing 0.5 % binder around the optimum, are presented in the graphs.

Figure 3-11 shows the FI results for Mix A and Figure 3-12 shows the results for Mix B. The data shows that, in both mixes, the FI increases with increased binder content and the increase is monotonic. Unlike what was seen in the BBR tests, no separate trend was seen when the binder content was below optimum; more binder simply increases the FI.

Comparing the results between the samples fabricated at CME to those fabricated at UDOT shows that while both show the same trend, there is a bias in the data with CME always resulting in a higher FI. The bias is relatively small for Mix A but becomes significant for Mix B; the reason for this bias is not known but it is further investigated in Section 5.

It is noted that the range of FI in Mix A ranges from around 4.2 at 4.1 % binder content to 11.8 at 5.1% binder content. The FI for Mix B ranges from around 13 at 4.75% binder content to near 30 at 5.75% binder content. While specific thresholds have not been developed for Utah environments, comparison of these values to values reported in the literature indicate that Mix A has low FI as tested and might be susceptible to fatigue cracking while Mix B is expected to show better performance. Both Mix A and Mix B are actual mixes placed around the Salt Lake City area but their field performance in fatigue has not been documented.

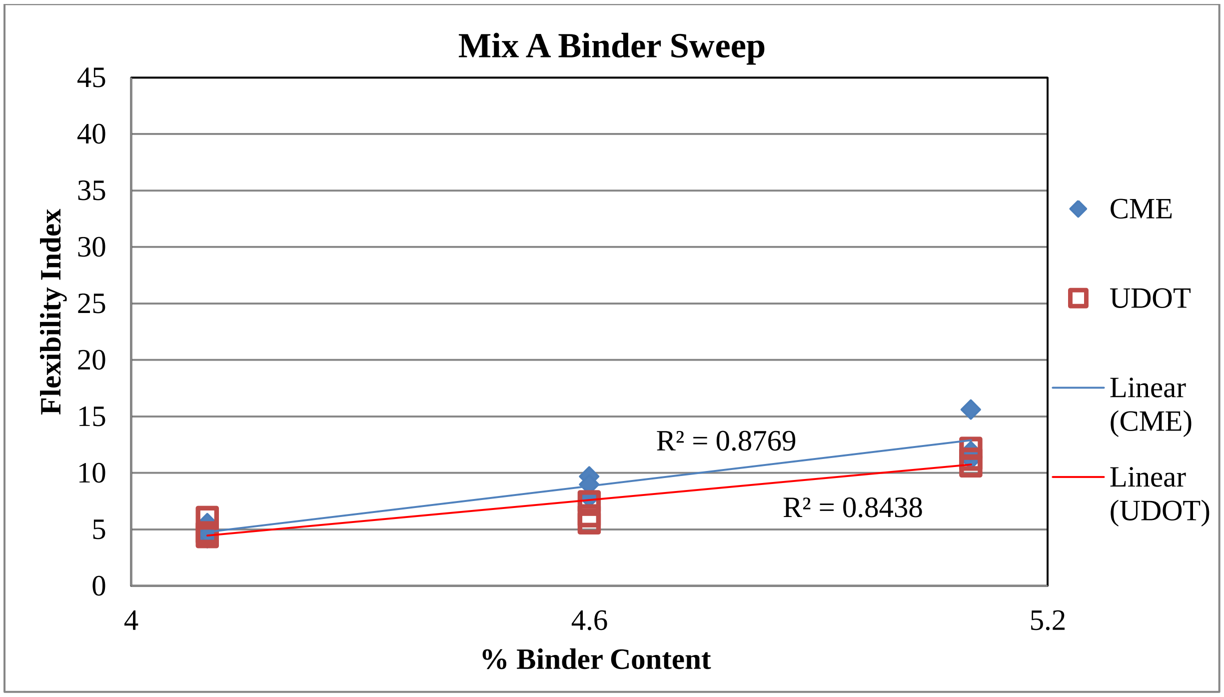

Figure 3-11 Effect of Asphalt Binder Content on Mix A

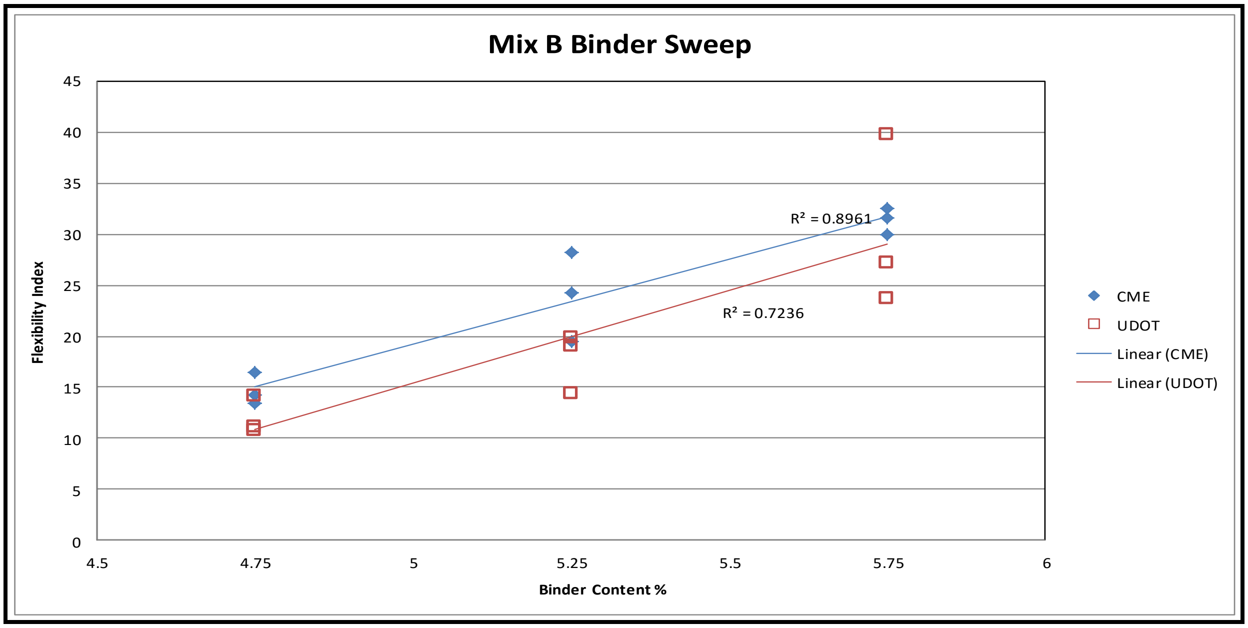

Figure 3-12 Effect of Asphalt Binder Content on Mix B

When comparing Figure 3-11 to Figure 3-12, the FI increases linearly with increasing binder content from 4.1% to 5.75%. While the slope for Mix A is different from the slope for Mix B, this indicates that perhaps a single trend can exists between binder content and FI.

3.3.2.1 Air Voids

AASHTO TP-124 states that the air voids of the samples should be 7 ± 0.5. This means that there can be up to a 1 percent different in air voids on different samples. To evaluate if this tolerance had any effect in the results, the FI as a function of air voids for the design target binder content was evaluated in Mix B. Since some variability in voids was present in the samples, a targeted sample set was not prepared. The random air voids were plotted against FI and the results are shown in Figure 3-13.

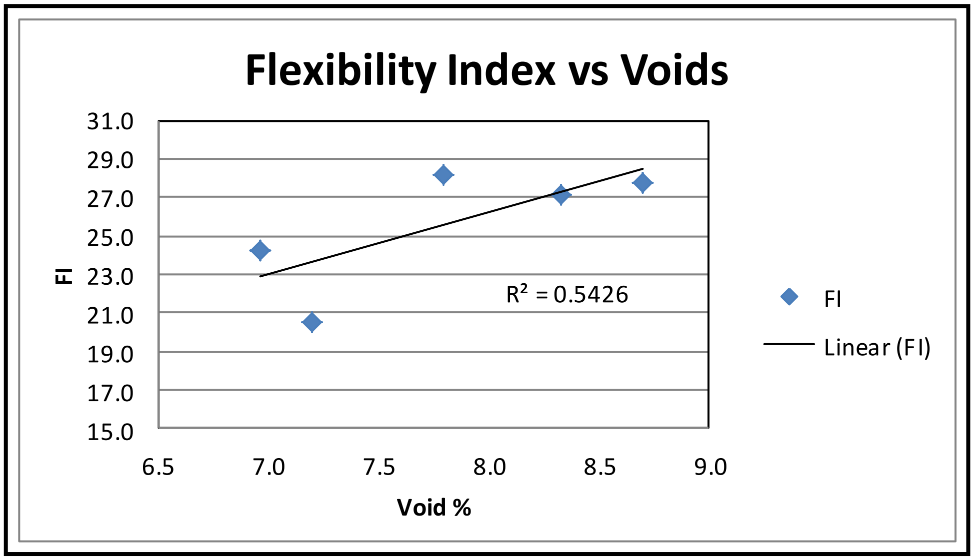

Figure 3-13 Effect of Air Voids on FI for Mix B

Figure 3-13 seems to indicate that higher void content might lead to higher FI. This finding is counterintuitive to common expectation because greater void content results in less volume filled with solids and thus lower energy to failure. Each air pocket is surrounded with surfaces requiring no energy to create; in effect, a crack requires no energy to be carried through this volume. Unfortunately, not enough data was collected to make a more definite conclusion.

3.3.2.2 IFIT Analysis

Both mixes show an increase in FI as binder increases. The coarse, low binder demand mixture (Mix A) developed a much lower FI than the finer, high binder demand mixture (Mix B). The increase in FI with binder content is relatively linear with an R^2 above 0.80 for both mixes. The two mixes exhibit nearly the same FI where the binder content between the low binder variant of Mix B (4.75%) and the high binder variant of Mix A (5.1%). The FI in this area is near 12 for Mix A and 13 for Mix B. Both slopes are around 0.8. This may, with further investigation, suggest a continuous relationship between FI and binder content under constant void conditions. However, this finding is confounded by the observation that by increasing voids filled with asphalt (VFA), there is a tendency toward lower FI.

A possible explanation of the lower FI for the higher VFA condition is the observation of broken aggregates in the more compacted mixture. Mix B may be reaching a lock point around 7.5% voids and the relationship is a step function with FI being 28 between 7.5 and 8.7% while being 22 below 7.5% void. This theory suggests that a density of 92.5% of theoretical maximum is too high for this mixture and aggregates are fractured below a 7.5% void threshold. More data is needed to verify if this assertion has merit.

3.4 Summary

3.4.1 BBR

Based on the analysis of the BBR results the following can be determined:

1. *60 and 120 second creep modulus from SGC samples varying compaction with binder content constant:* From beams measuring 0-2% air voids compared to beams with greater than 8% air voids, creep modulus roughly decreases by 30%. The 120 second creep modulus follows the same trend.
2. M-values at 60 and 120 seconds are not affected by air void content.
3. *60 and 120 second creep modulus from SGC samples varying binder content with compaction level held constant:* The creep moduli are approximately constant with binder contents close to the optimum of the mixture design. At great deficiencies or excessive quantities of binder contents, creep modulus values differ significantly. A greater difference in creep modulus is seen in mixes deficient in binder content compared to mixes with excessive binder content. A mixture deficient in binder content can have decreased results on the magnitude of 30% while a mixture with excessive binder content will have a difference of about 15% or half of the deficient binder mix.
4. M-value is independent of binder content.

3.4.2 IFIT

Based on the analysis of the FI, the following can be determined:

1. Both mixes A and B show an increase in FI as binder increases.
2. A single relationship between FI and binder content may exist due to both the monotonic increase and the similarity of FI at the same binder content in both mixes.
3. Although the IFIT test results are not indicative of any specific material property, the test seems to be able to detect changes in air voids and changes in binder content.

4. It appears that some relation exists between lower air voids and lower FI. This may not be as it appears; there is indication of a step relationship with the step to lower FI occurring around 7.5% air. More data is needed to evaluate this relation.

3.4.3 Combined Tests Observations

By looking at the results from the BBR and the IFIT, it is clear that increases in binder content are beneficial to the overall performance of the mixture (at least at low and intermediate temperatures). As the binder content increases, the BBR results show a slight decrease in creep modulus; this condition is associated with better performance. As the binder content increases, there is an increase in the FI which is also a condition associated with better performance. Deficiencies in binder content seem to be a problem for the BBR results as they indicate a desirable condition (lower modulus, same m-value), which is contrary to accepted knowledge. The IFIT clearly shows that deficiencies in binder content would result in decreased expected performance.

While the FI seems to be a more sensitive parameter than the creep modulus or m-value to changes in binder content; the reverse is true for air voids. A decrease in creep modulus was measured with increased air voids but only a step function was seen in the FI. It should be noted, however, that the change in air voids in the BBR experiment range from zero to ten percent while the variation in air voids for the IFIT tests was limited in range from seven to nine percent. A better designed experiment should be conducted in the IFIT to evaluate the effect of voids.

While both tests show variations in results with changes in volumetrics (binder content and air voids), neither of these tests is expected to be used for volumetric verification as there are better tools available for this purpose. However, the results indicate that adoption of the IFIT would likely result in mixtures with higher binder content being favored during design; no such changes would be expected with the adoption of the BBR.

4.0 EFFECT OF RAP AND AGING

4.1 Overview

In this part of the study, the effect of RAP and aging on the low-temperature performance of asphalt mixtures were investigated using the mixtures described in Section 2.3. Aging and RAP content were studied together given that the binder in the RAP has already been aged in the field and it is common practice to assume that a portion of that binder will blend with the virgin binder. The process and amount of blending that actually occurs is not well understood but will depend, among other factors, on the temperatures that the mixtures are subjected to. The same elevated temperatures will also age the virgin binder.

Understanding the effects of aging in asphalt binders and how the virgin binder is replaced with aged material is important for controlling the low and intermediate temperature cracking behavior of pavements. It is believed that increasingly aged binders have detrimental effects in the performance of asphalt mixtures once placed in the field; therefore, any test used in asphalt mixtures must be able to capture the addition of RAP and progressive aging. In this study, an experimental matrix, shown in Table 4-1, was developed to look into increased aging and aged binder replacement.

Table 4-1 Experimental Matrix

Binder	**Gradation**	**Aggregate Type**	**RAP, %**	**Aging Protocols**	
				Loose Mixture At 135 ºC, hours	Compacted Mixture At 80 ºC
PG 64-28	A 19mm NMAS	Limestone	0, 15, 25, 35	0, 3, 6	48, 120, 168 hours (2, 5, 7 days)
	B 12.5 mm NMAS	Granite			

4.2 BBR Results

For the low temperature part of this study, forty-eight mixture pucks were prepared using standard procedures for Superpave Gyratory Compacted (SGC) asphalt mixtures and tested as described in Section 2.2.1. The samples were made using varying RAP content and laboratory aged for different intervals both before and after compaction as shown in Table 4-1.

4.2.1 Procedures

As shown in Table 4-1, three RAP contents: 15%, 25%, 35% were selected for this study in addition to the normal control mixtures, which are designated as 0% RAP mixtures. To investigate the effect of long-term aging, the samples were subjected to two different temperatures either before or after being compacted. For those being aged prior to compaction (i.e., loose mix), a temperature of 135^{o}C was used, the mixtures were aged for additional 3 hours and 6 hours before compaction. These mixtures are called loose mixtures. The rest of the mixtures were compacted and then placed inside a forced-draft oven at 80 ^{o}C for periods of 2, 5, or 7 days. Following the aging protocols, the compacted samples were then cut into beams for BBR testing. With four different RAP contents and six different aging periods, 24 different combinations of mixtures were obtained for each aggregate source, and therefore, a total 48 asphalt concrete mixtures were used for this part of the experiment.

4.2.2 Results

A summary of results of the effect of aging for different RAP content are shown on APPENDIX B: DATA,Table 0-1 and Table 0-2. As can be seen in the tables, the data is very consistent; in all cases, the coefficient of variation (standard deviation divided by the mean) was below 15% and quite often below 10% for both the modulus and the m-value. This is consistent with previous reports and is an indication of the quality of the results, the easy of testing, and the reliability of the test.

The data for each condition was plotted showing the change in creep modulus and the change in m-value for each of the mixtures tested. No error bars are shown on the figures but, as previously stated, the coefficient of variation was below 15%.

The results in Figure 4-1 show that, as the RAP content increases, the creep modulus also increases at each aging condition. The increase in Mix A's creep modulus to the addition of 35% RAP is almost 30% (Figure 4-1-b) while Mix B shows an increase in creep modulus of almost 50% for the same RAP content (Figure 4-1-d). This indicates that the interaction between RAP and virgin material is probably mixture dependent. Mix B has more binder than Mix A, thus it is not unreasonable to expect greater changes. It could be argued that binder replacement (i.e., less virgin binder in the mix and not complete blending) could be responsible for some of the changes observed. However, it was shown in Section 3.2.3 that the magnitude of the change in the modulus is not likely from a change in binder content alone; therefore, the changes observed are the results of aging the binder and some blending of the RAP with the virgin mix.

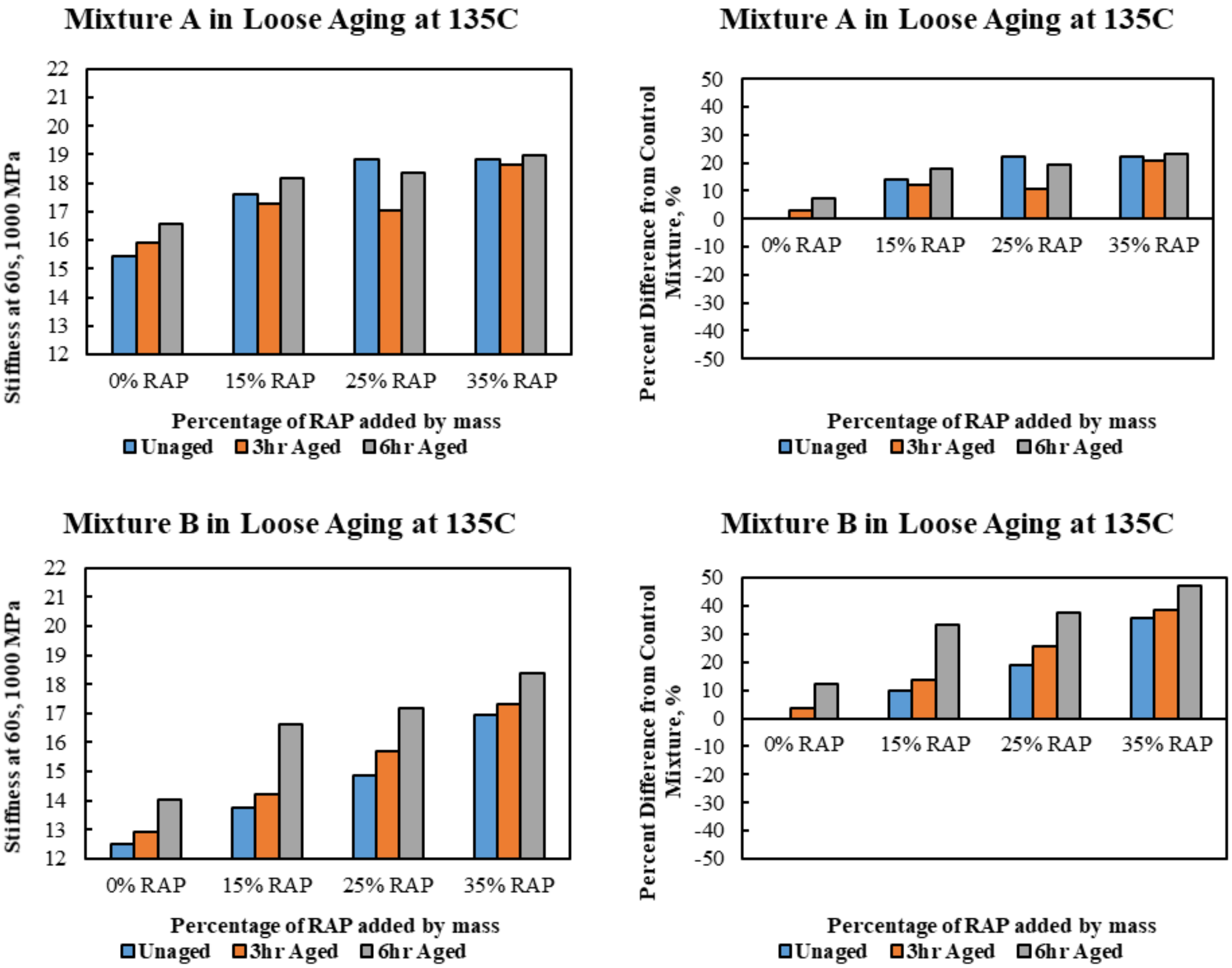

Figure 4-1 a-d Effect of RAP on Creep Modulus for Different Aging Times

Aging of the loose mixture at 135 °C for 3 or 6 hours results in an increase of modulus regardless of the RAP content. However, Figure 4-1 a and b show that, when RAP is added to Mix A and the loose mixture is aged, a reduction in creep modulus can be observed between the unaged to the 3 hour aged condition. The reason for this is not clear but it is not believed that it represents an improvement in expected performance. Perhaps, this behavior could be caused by loss of cohesion from the loss of volatiles in the binder. As was discussed in Section 2.3, Mix A is coarser mixture with lower binder content as compared to Mix B. Mix A also has an overall higher creep modulus so perhaps there is a limiting or asymptote value around 18,000 MPa that must be considered.

Figure 4-2 shows results for the m-value. The data shows that an increase in RAP decreases the m-value and, just like was seen for the modulus, the effect of loose mixture aging is not consistent for Mix A (Figure 4-2 a and b); but a consistent decrease in m-value for Mix B is seen with increased RAP content (Figure 4-2 c and d).

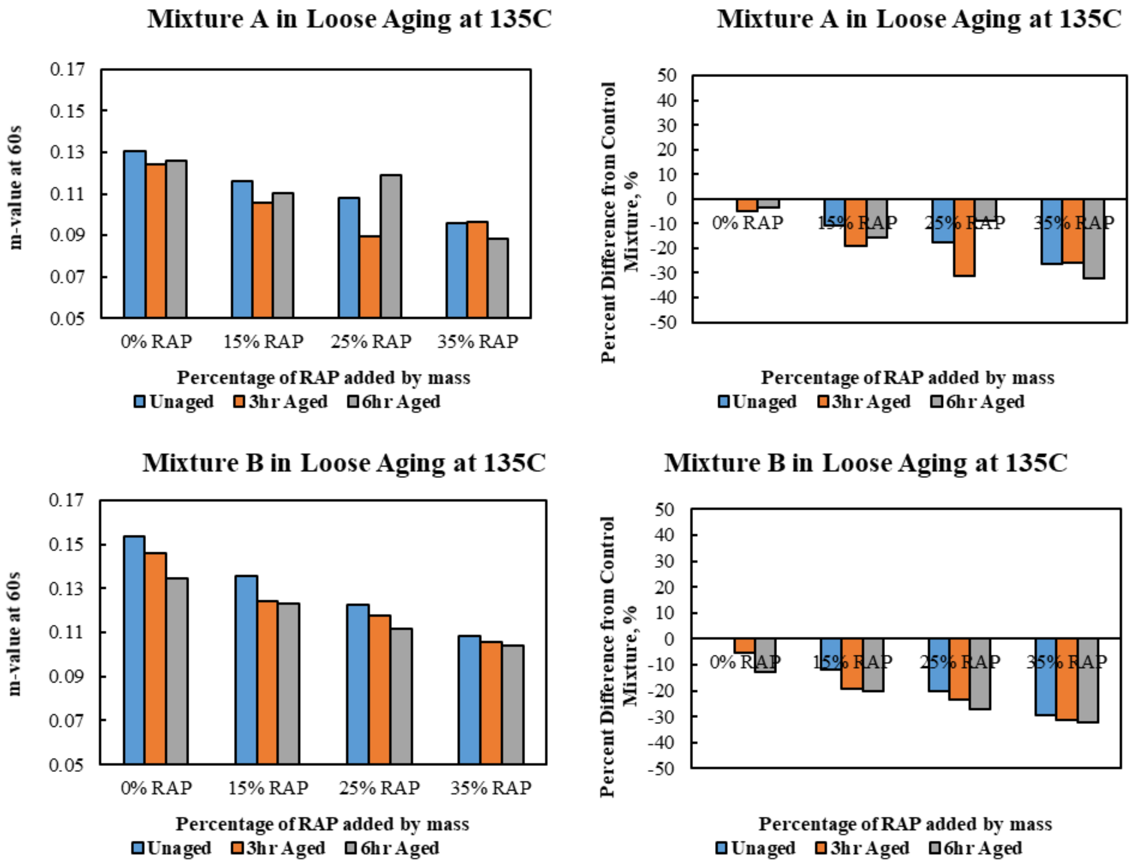

Figure 4-2 a-d Effect of RAP on m-value for Different Aging Times

When evaluating the overall trend, it is evident from the results that adding RAP to a mixture increases the creep modulus AND decreases the m-value. These changes mean that even a moderate amount of RAP, as low as 15%, can be captured by the BBR tests. The tests predicts that the addition of RAP is detrimental to the low temperature mixture performance.

Figure 4-3 shows the effects of increased RAP content on the creep modulus but with aging done on the compacted samples at 80 ºC. Mix A shows some scatter in the results with some cases having a decrease in modulus after aging (Figure 4-3 a). For example, mixtures with 15% and 25% RAP have a lower modulus after 7 days of oven aging than the same mixtures with no aging. Mix B shows a consistent trend of increased modulus with increased RAP content. It is believed that the scatter observed in Mix A is related to the lower binder content.

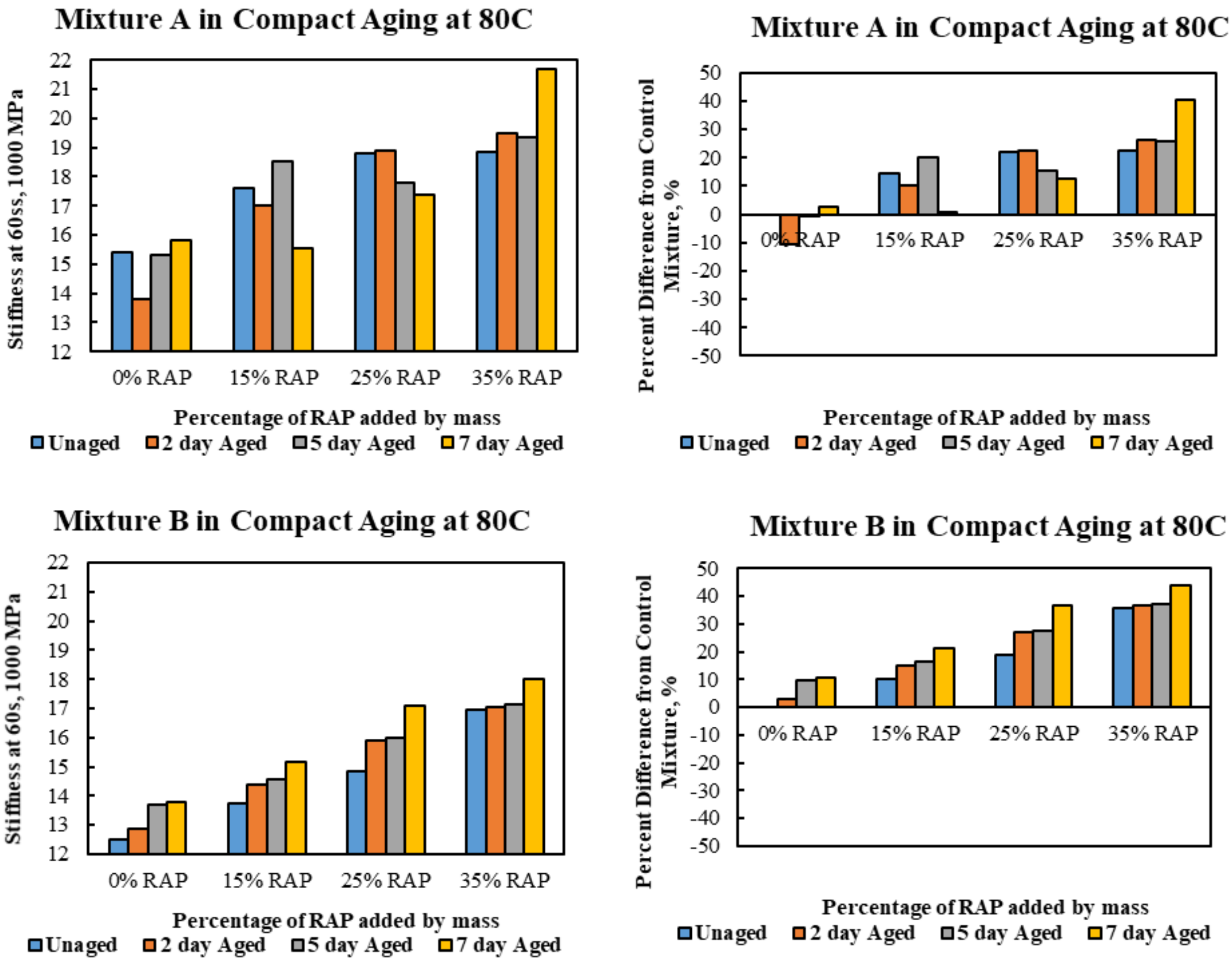

Figure 4-3 a-d Effect of RAP on Creep Modulus at Different Aging Days

Figure 4-4, shows the changes in the m-value from oven aging and increased RAP content. This parameter decreases with oven aging time and increased RAP content for both Mix A and Mix B. Evaluating both modulus and m-value leads to the conclusion from oven aging of compacted mixtures that, as RAP is added to the mix, a decrease in performance is expected.

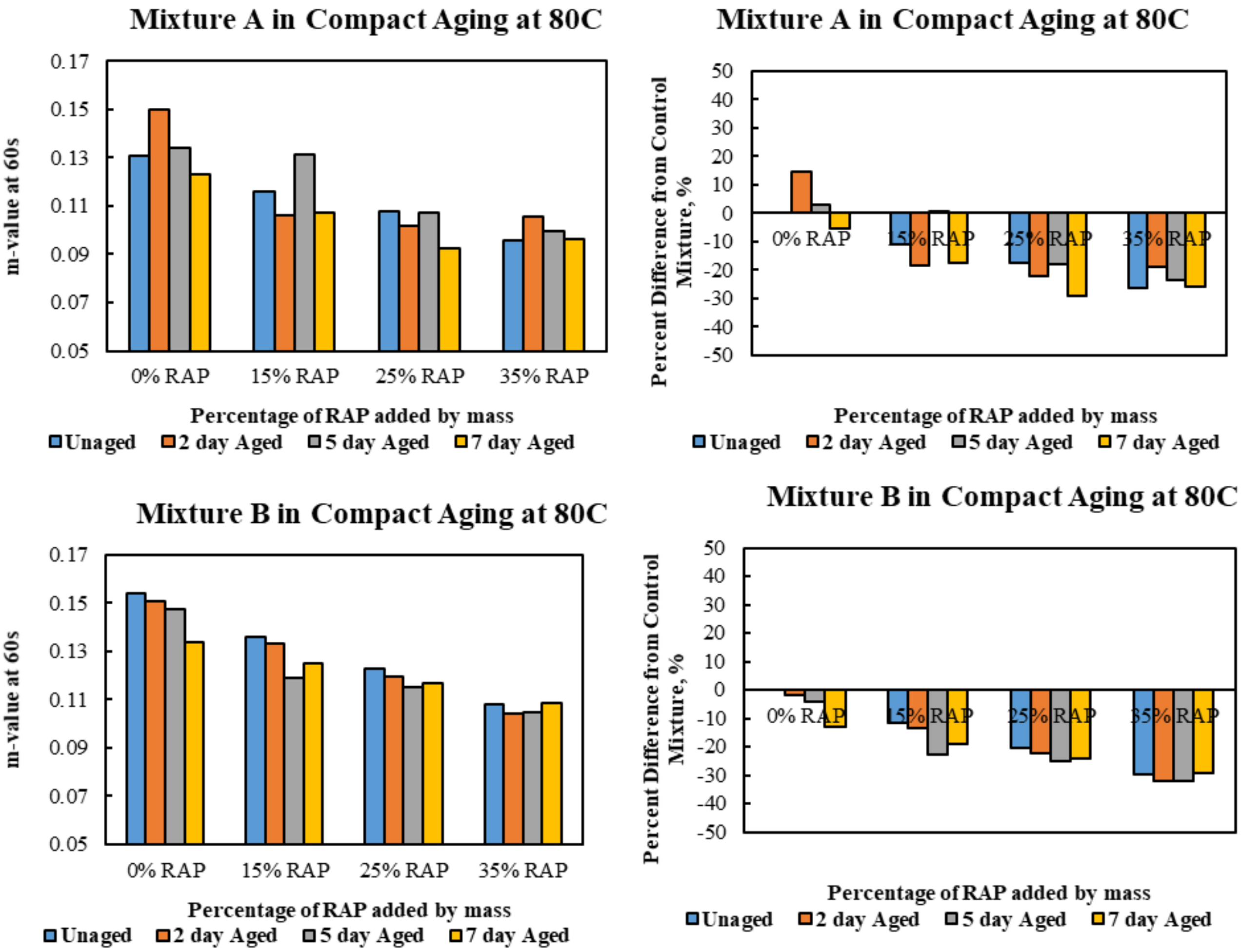

Figure 4-4 a-d Effect of RAP on m-value for Different Aging Days

4.2.2.1 Practicality of Aging Procedures

Based on this experiment, and from a practical perspective, aging of the loose mixture at 135 ºC is preferable to aging the compacted mixture at 80 ºC since loose mixture aging conditions the material in a much shorter time while yielding similar conclusions, albeit different numbers, for creep modulus and m-value. An equivalency between both aging methods can be determined; however, to develop such a relation, the combined effect of change in modulus and change in m-value must be understood. This is investigated in the next section.

4.2.3 BBR Analysis

The results shown in the previous section indicate that both the creep modulus and the m-value are adversely affected by increases in RAP content and aging conditioning. In order to gain a better understand of the process, the two variables -modulus and m-value- were combined into a single index value. Previous work has shown that both values play a role in mixtures performance so, for this analysis, the changes in both values were given the same weight (i.e., a 10% increase in modulus has the same effect as a 10% decrease in m-value). This assumption needs to be verified with further studies but it would not change the observed trends.

The index value is determined as the absolute difference between the given condition (RAP content, Aging time/condition) and the control condition (no RAP, no Lab Aging) for that mixture. It considers both the change in creep modulus and the change in m-value.

The Index is calculated based on the following equations,

$$\boldsymbol{\Delta_{modulus}} = \frac{\boldsymbol{Modulus_{time/RAP} - Modulus_{Control}}}{\boldsymbol{Modulus_{Control}}} \qquad \textbf{Equation 4-1}$$

$$\boldsymbol{\Delta_{m-value}} = \frac{\boldsymbol{m{-}value_{time/RAP} - m{-}value_{Control}}}{\boldsymbol{m{-}value_{Control}}} \qquad \textbf{Equation 4-2}$$

$$\boldsymbol{Index} = \sqrt{(\boldsymbol{\Delta_{Modulus}})^2 + (\boldsymbol{\Delta_{m-value}})^2} \qquad \textbf{Equation 4-3}$$

The data was separated into two graphs, RAP content for different aging conditions (Figure 4-5 and Figure 4-6) and aging time for different RAP contents (Figure 4-7 and Figure 4-8). While this is essentially the same data just plotted with a different X-axis, the Index was labeled as RAP Index and Aging Index, respectively, to separate the different treatments and try to better understand their effect.

Figure 4-5 and Figure 4-6 show a linear relation between RAP content and RAP Index. A regression line resulted in very high r-squared values (97% or higher). It should be noted, however, that the intersect of the regression equations was not forced through zero; this is the results of using the control mix as a reference for all cases. Thus, only the slope of the line will be discussed as it represents the overall (modulus and m-value) rate of change caused by each variable studied. For clarity, only two conditions are shown with regression lines.

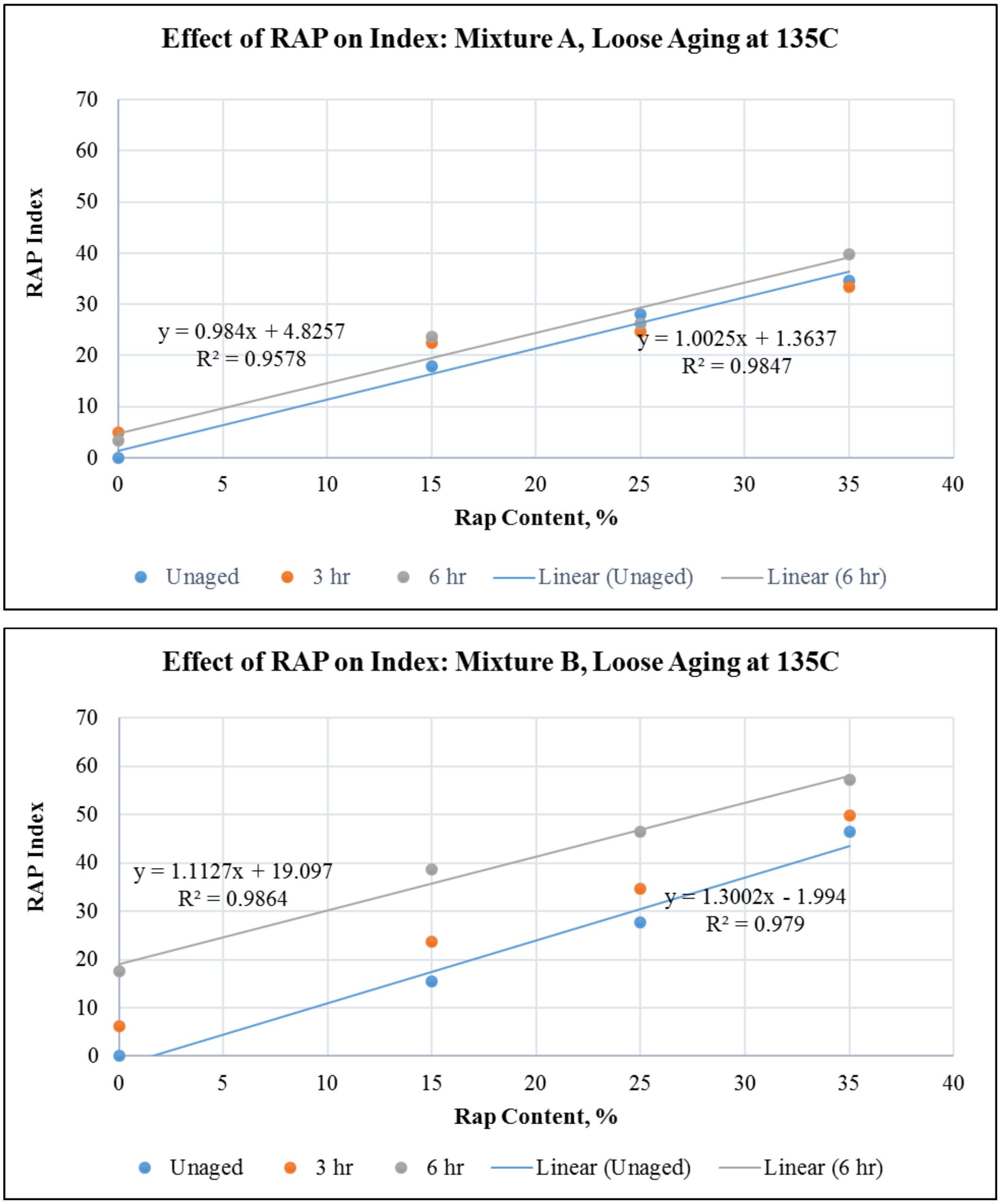

Figure 4-5 a-b Effect of RAP content on Index for Loose Mix Aging

Figure 4-5 shows the RAP Index as a function of RAP content for different loose mixture aging condition times. Mix B shows higher sensitivity for RAP having a slope for the unaged condition of 1.3 versus 1.0 for Mix A. For 6 hours of aging the slopes were 1.1 for Mix B versus

0.98 for Mix B. However, as was shown in Figure 4-1, Mix B has a lower creep modulus than Mix A with no RAP and no aging (12,000 MPa vs 15,000 MPa) and higher m-value (Figure 4-2). The data suggests that the starting value of modulus and m-value for the baseline condition has an influence on the rate of change.

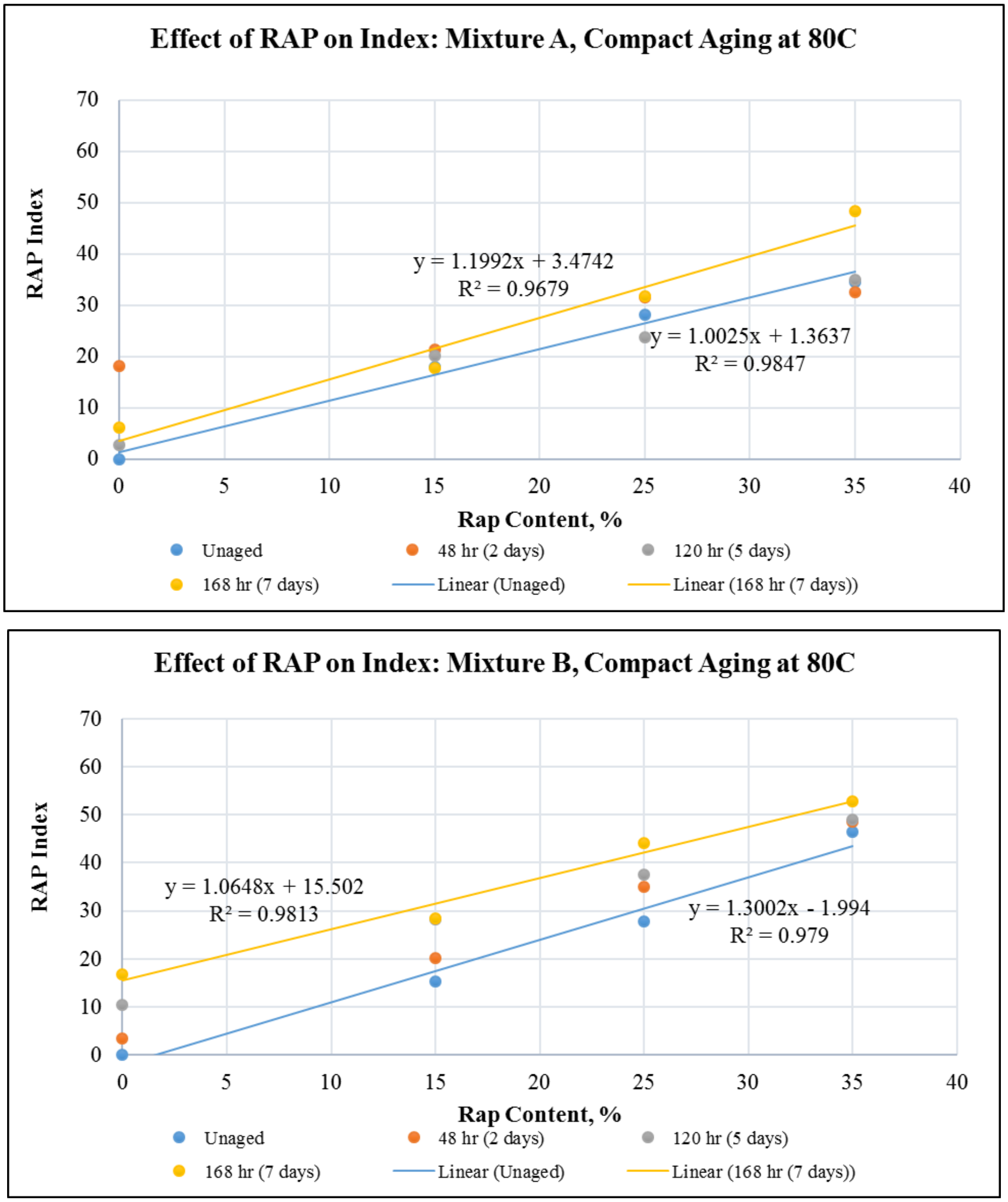

Figure 4-6 a-b Effect of RAP Content on Index for Compacted Aging

Figure 4-6 shows the effect of RAP content on the RAP Index for different compacted aging times. For the unaged condition, Mix B has higher sensitivity to the addition of RAP than

Mix A with a slope of 1.3 versus 1.0; however, after 120 hours of aging at 80 ºC the role reverses with Mix A now having a slightly higher slope of 1.2 versus 1.1. The sensitivity of this index is not known; therefore, no statement is made regarding the significance of such change.

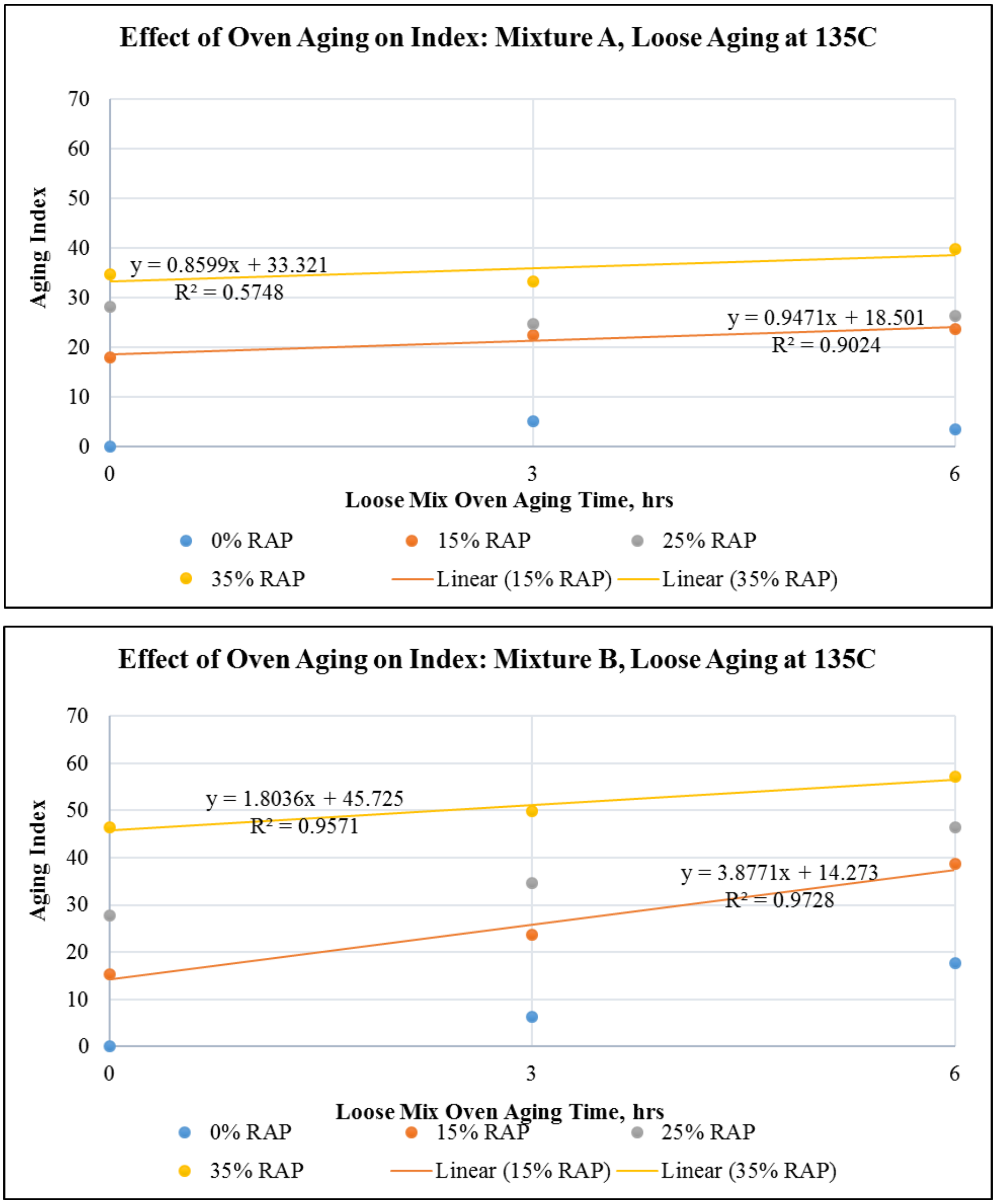

Figure 4-7 a-b Effect of Loose Mix Aging on Index for Different RAP Contents

Figure 4-7 shows the Aging Index as a function of loose mixture oven aging time at 135 ºC. Mix A shows a lower sensitivity to aging time with a slope of 0.9 while Mix B shows a slope of 3.8 for 15% RAP and 1.8 for 35% RAP. As in the case with the RAP Index, it seems that a mixture that starts with low performance expectations (high modulus and low m-value) would not change dramatically as compared to a mixture with good performance expectation. This was previously discussed in Section 4.2.2.

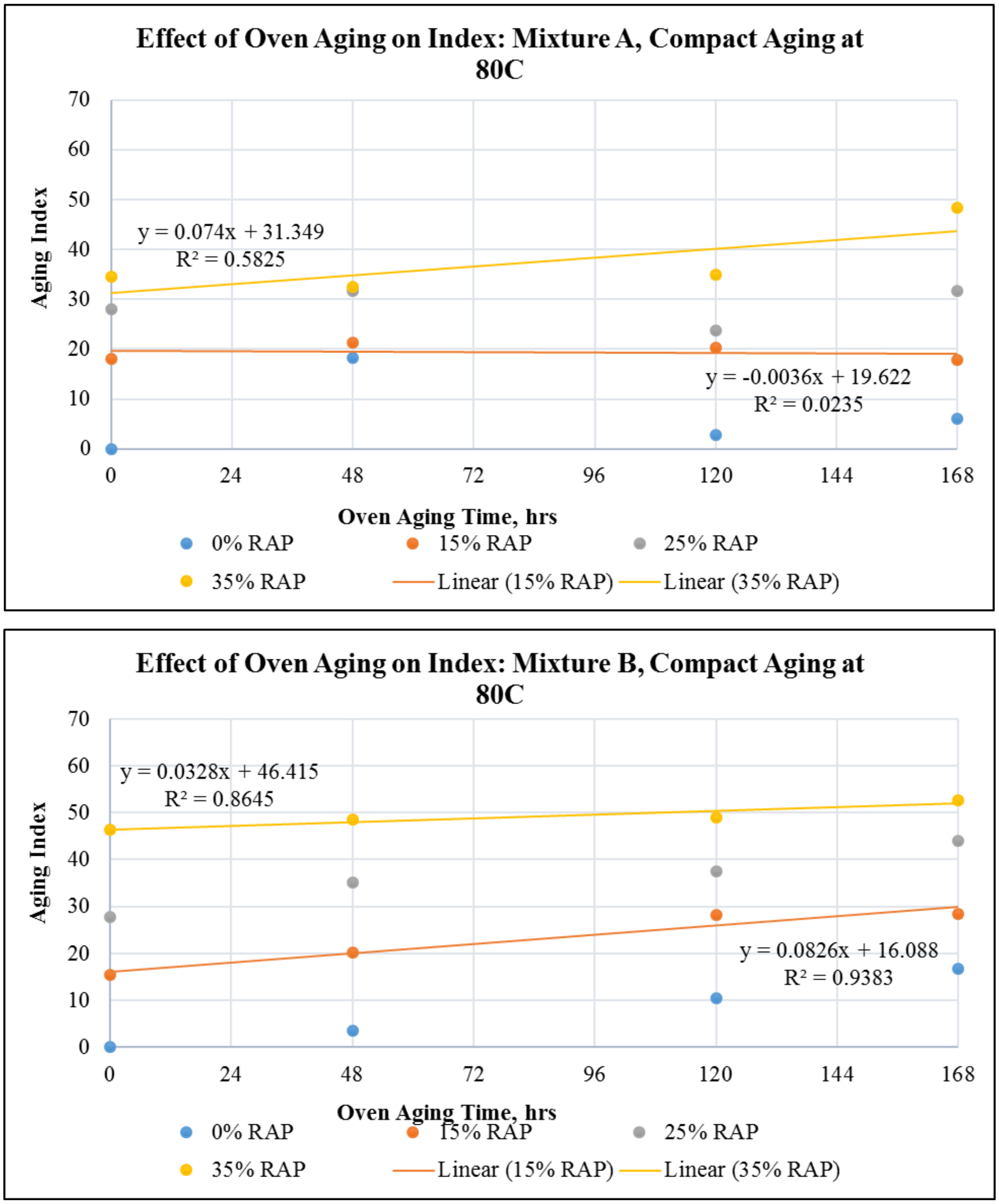

Figure 4-8 a-b Effect of Compacted Aging on Index for Different RAP Content

Figure 4-8 shows Aging Index as a function of compacted aging time. As was seen in Section 4.2.2 Mix A shows significant more scatter in the results resulting in a low r-squared for the regression line. The low value for the slope of the regression in both mixes show that there is low sensitivity to this type of laboratory aging. The lower temperature and the fact that the mixtures are compacted might make it more difficult for the blending of RAP and virgin material to occur and for the volatiles in the virgin material to change.

Of interest is a comparison of the effects of aging conditioning of loose mixture versus compacted mixes. As was mentioned in Section 4.2.2.1 there is a significant advantage, from a time perspective, in aging the mixture before compaction than aging it after compaction; furthermore, the results indicate that aging of loose mixtures induces more changes in the BBR parameters than aging of compacted specimens in a shorter amount of time.

By comparing Figure 4-7b and Figure 4-8b for 35% RAP (the most clear data), the equivalent time of compacted aging at 80 ºC required to obtain the same Aging Index for 1 hour of loose mixture aging at 135 ºC can be calculated as 55 hours (1.8036/0.0328). For no RAP this value is 47 hours (3.8771/0.0826). This shows the advantage of loose mixture aging versus compacted mixture aging when time is a concern. Furthermore, loose mixture aging shows less variability than compacted aging and, even though the higher temperature might lead to chemical changes in the asphalt binder, the fact that the mixture is already at the compaction temperature makes this option very more attractive for everyday use.

4.3 SCB IFIT Results

For the intermediate temperature part of this study, thirty mixture pucks with 120 tests were made using the procedures described in Section 2.2.2.1 and tested as described in Section 3.3.1. The samples were made using varying RAP content and then laboratory aged for different intervals following the experimental matrix shown in Table 4-1. Aging was done on compacted samples in accordance with AASHTO R-30.

4.3.1 IFIT Procedures

Three replicate samples of each condition listed in Table 4-2 were prepared and tested in the same manner as has been previously described.

Table 4-2 Aged/Replacement Binder Testing Matrix

	RAP Content			**Compacted Aging AASHTO R-30**	
Mix A	15%	25%	35%	Short (2 hr)	Long (120 hr)
Mix B					

4.3.2 IFIT Results

The specimen properties for the IFIT results are shown in APPENDIX B: DATA. For each condition 4 samples were run; the data from the highest strength sample was dropped and the FI was calculated for the remaining three. The three FI values were averaged and this average is presented on this section.

Figure 4-9 and Figure 4-10 show the effect of RAP content on the FI. For both Mix A and Mix B there is a decline in the FI with the addition of RAP. There is also a decrease in FI between short term aged samples and long term aged samples; however, at 35% RAP, there is no FI difference between the unaged binder/RAP blend and the long term aged binder/RAP blend. As was observed in the binder sweep, the low binder demand design (i.e., Mix A) begins with a low FI and, as RAP is increased, the index drops. For Mix A, the difference between the unaged virgin mixture and the 120 hour aged mixture is a drop in FI of about 33 percent from 9 to 6. For Mix B, the difference between the unaged virgin mixture and the 120 hour aged mixture is a drop in FI of about 10 percent from 20 to 18.

The figures also show that there is a bias between results produced by UDOT and CME even though the same equipment was used. For the same condition, CME results were consistently higher. The reason for this bias is not known but a more detailed discussion on the variability of the results is presented in Section 5.0.

Of interest is the fact that, at low FI values, the difference between different conditions decreases. It seems that as the FI reaches a value below 10 or so the results seem to reach an asymptote. This is similar to the observation described for BBR data. It is speculated that a certain stiffness is the cause of this data compression. Further analysis of the relation between the sample stiffness and the FI may provide more information regarding this issue.

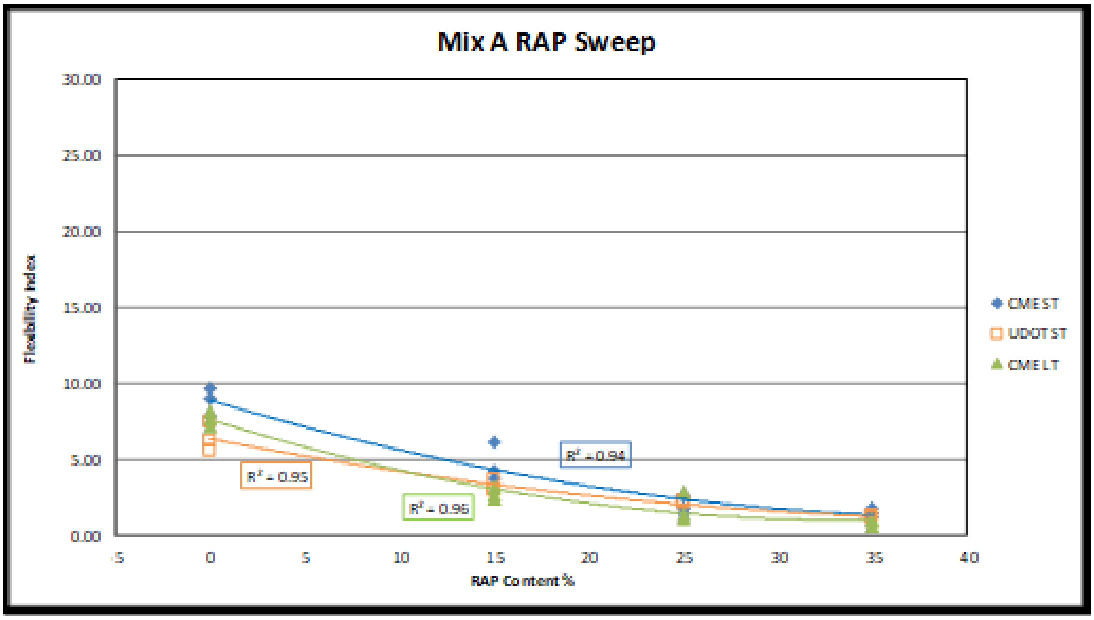

Figure 4-9 Mix A, RAP and Long Term Aging Sweep Results

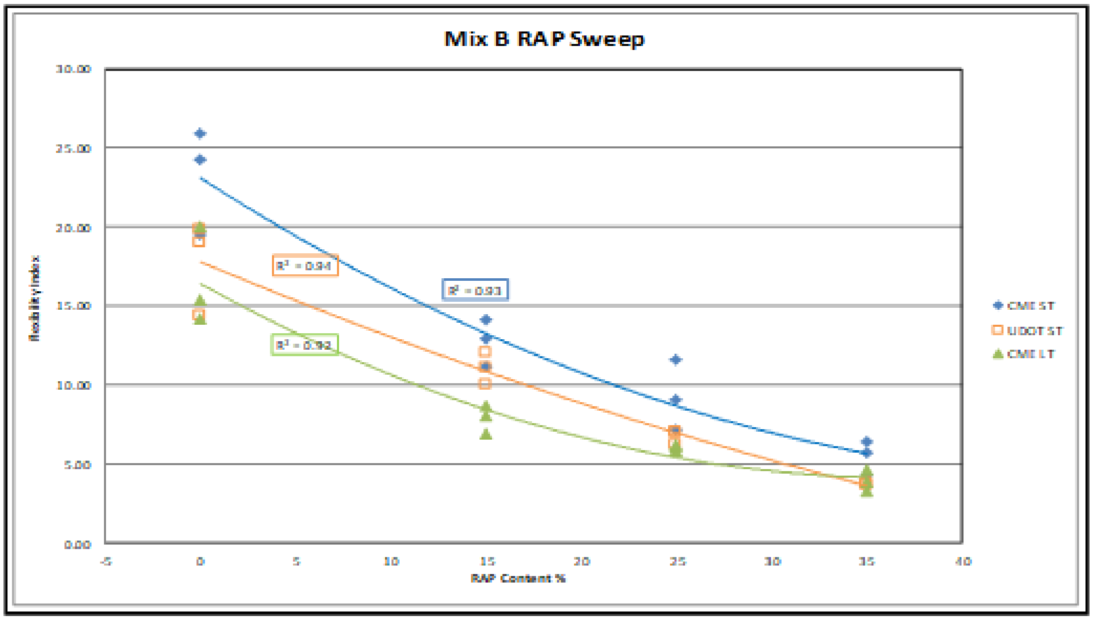

Figure 4-10 Mix B RAP and Long Term Aging Sweep Results

4.4 Summary

In this section, samples were prepared with different amounts of RAP and aged for different periods both before and after compaction. Both tests (BBR and IFIT) show a decrease in expected performance with the addition of RAP and with increased aging time.

4.4.1 BBR Summary

The following results were obtained from BBR testing.

1. Laboratory aging produced significant changes in the modulus and m-value of the asphalt mixtures and should be considered during mixture design.
2. Two different aging procedures were evaluated and loose mixture aging at 135 ºC gave the most consistent results in a reasonable amount of time.
3. Based on one of the mixes studied, one hour of loose mixture aging at 135 ºC provides the same change in material properties as 47 to 55 hours of aging of the compacted mixture at 80 ºC.
4. The introduction of RAP to the mixture adversely affect both the modulus and the m-value of the mixes studied, however, the magnitude of the changes is mixture specific.\ and probably related to overall binder content.
5. Changes in modulus and m-value can be combined into a single index. This index is linearly related to the amount of RAP introduced to the mix.
6. The mixture with the high modulus (Mix A) had the smallest change in properties when RAP was introduced or when aged in the lab. The mixture with the low modulus (Mix A) had the largest change in modulus or m-value; however, the fact that the modulus was relatively low for the control condition indicates that this mixture should have acceptable performance once placed on the field.

4.4.2 IFIT Summary

The following observations are obtained from IFIT testing:

1. Increasing RAP content decreases FI in both mixes.

2. As the RAP content increases, the FI decreases at a decreasing rate and at 35% RAP there is little difference between an unaged RAP blend and an aged RAP blend.
3. The greater the binder content, the less aging affects the mix.
4. FI seems to be an indicator of toughness above a FI value of around 10 but below that value the data seems to compress. This may indicate a reduction in sensitivity as the modulus of the material increases.
5. FI is not an indicator of fundamental material properties but seems to pick up differences in the overall age of the binder.
6. Some source of bias exists between the results of the two labs with CME always showing higher results than UDOT for the same conditions.

4.4.3 Combined Tests Summary

The data from IFIT and BBR indicate aging causes mechanical changes in the material that relate to lower performance. The tests also indicate that RAP is detrimental to the overall expected performance of the mixtures when compared to virgin mix. However, the data from the IFIT test indicates an asymptote as age increases and as RAP content increases but the data from the BBR shows no such trends. Based on this observations, the BBR appears to be a more sensitive test to capture the effect of aging and RAP on the material.

Conditioning the loose mixture at 135 ºC prior to compaction seems to be a practical method to accelerate the effect of aging when compared to conditioning the compacted specimen at 80 ºC. Even though 135 ºC could change the chemical composition of the binder, from the mechanical response, an equivalency can be established between field aging and laboratory aging that balances rigor and practicality.

5.0 SCB IFIT VARIABILITY

5.1 Introduction

Many measurements were recorded in the course of preparing and testing the samples for the tests as documented on this report. Many samples are paired between two labs, UDOT and CME, but some are not. Furthermore, the data analyzed in this section is produced under the limitations of AASHTO TP-124. Most of the samples met the requirements set forth in the standard but a few did not. This section compares a number of fabrication metrics between laboratories where paired samples exist. Some of the metrics result from fabrication on the same equipment by different technicians and some result from different equipment being used by different technicians. All of these sample pairs were produced within a week of each other. The Mix A binder sweep being the earliest and the Mix B RAP sweep being the latest.

5.2 Repeatability/Reproducibility

Repeatability is an in-lab question, reproducibility is a multi-lab challenge. Since all cutting, specific gravity testing and FI testing were done in one lab by two different technicians, evaluation of the repeatability of a single technician's work is possible while data for the reproducibility of the two technician's work is available without the confounding effects of multiple pieces of equipment. Final FI results provide insight into the repeatability of puck preparation. The following factors were measured for both repeatability and reproducibility, their specified limits from AASHTO TP-124 are included as a reference.

- Sample Thickness, explicitly 50 ± 1-mm
- Notch Depth, explicitly 15 ± 1-mm
- Ligament Length, implicit, calculated from radius and notch depth 59.5 ± 2mm
- Radius, implicit, 74 ± 1-mm depends on saw blade width
- Void Content, explicit 7 ± 0.5-mm

The metrics which are explicit appear to be critical geometric elements required in the measurement of the fracture curve. Implicit metrics such as radius and ligament length affect only the extreme tail of the curve; this area of the curve is also affected by a number of other factors including the compression stress field. The force/strain data collected in this area has only minor effect on the calculated index.

5.3 Results

All of the data used to create these evaluations can be found in APPENDIX B: DATA. The number of pairs for each set is 36. Individual technician tests are evaluated in Table 5-1, Table 5-2, Table 5-5, and Table 5-6. Multi-lab tests are evaluated in Table 5-3, Table 5-4, Table 5-7, and Table 5-8. Statistical methods of comparison are Average, Maximum, Minimum, Range, Sample Standard Deviation, Coefficient of Variation.

Table 5-1 Individual Technician Comparison, Mix A Binder Sweep

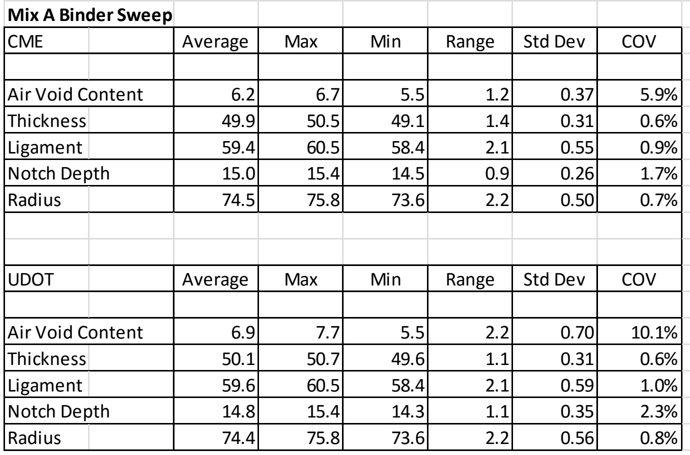

Mix A Binder Sweep						
CME	Average	Max	Min	Range	Std Dev	COV
Air Void Content	6.2	6.7	5.5	1.2	0.37	5.9%
Thickness	49.9	50.5	49.1	1.4	0.31	0.6%
Ligament	59.4	60.5	58.4	2.1	0.55	0.9%
Notch Depth	15.0	15.4	14.5	0.9	0.26	1.7%
Radius	74.5	75.8	73.6	2.2	0.50	0.7%
UDOT	Average	Max	Min	Range	Std Dev	COV
Air Void Content	6.9	7.7	5.5	2.2	0.70	10.1%
Thickness	50.1	50.7	49.6	1.1	0.31	0.6%
Ligament	59.6	60.5	58.4	2.1	0.59	1.0%
Notch Depth	14.8	15.4	14.3	1.1	0.35	2.3%
Radius	74.4	75.8	73.6	2.2	0.56	0.8%

Table 5-2 Individual Technician Comparison, Mix A RAP Sweep

Mix A RAP Sweep						
CME	Average	Max	Min	Range	Std Dev	COV
Air Void Content	6.37	7.4	5	2.4	0.64	10.0%
Thickness	50.44	61.5	49.5	12	2.53	5.0%
Ligament	60.06	61.4	59.0	2.4	0.62	1.0%
Notch Depth	14.46	16.2	13.8	2.4	0.41	2.8%
Radius	74.51	75.6	73.3	2.3	0.64	0.9%
UDOT	Average	Max	Min	Range	Std Dev	COV
Air Void Content	7.5	8	6.6	1.4	0.38	5.1%
Thickness	49.7	50.2	49.1	1.1	0.26	0.5%
Ligament	60.2	61.1	59.2	1.9	0.47	0.8%
Notch Depth	14.2	14.9	13.9	1.0	0.20	1.4%
Radius	74.4	75.28	73.45	1.8	0.41	0.6%

Based on the comparison presented in Table 5-1 and Table 5-2, the following observations are noted for each individual lab.

CME

- air voids: both cases, low with excessive scatter
- thickness: target with excessive scatter and greater value than allowed for binder sweep
- ligament: on target with excessive scatter for binder sweep
- notch depth: on target with excessive scatter for RAP sweep
- radius: slightly high with excessive scatter

UDOT

- air voids: slightly low for binder sweep and high for RAP sweep with excessive scatter
- thickness: on target but with excessive scatter
- ligament: high for RAP sweep with excessive scatter
- notch depth: low for RAP sweep with acceptable variation
- radius: slightly high for binder sweep with excessive scatter

Table 5-3 Multi Lab Comparison, Mix A Binder Sweep

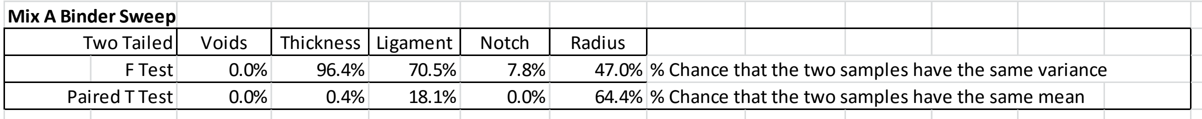

Mix A Binder Sweep

Two Tailed	Voids	Thickness	Ligament	Notch	Radius	
F Test	0.0%	96.4%	70.5%	7.8%	47.0%	% Chance that the two samples have the same variance
Paired T Test	0.0%	0.4%	18.1%	0.0%	64.4%	% Chance that the two samples have the same mean

The results of the paired t-test indicate that, for the binder sweep, only the radius has a probability greater than 60% that both labs are producing the same value.

Table 5-4 Multi Lab Comparison, Mix A RAP Sweep

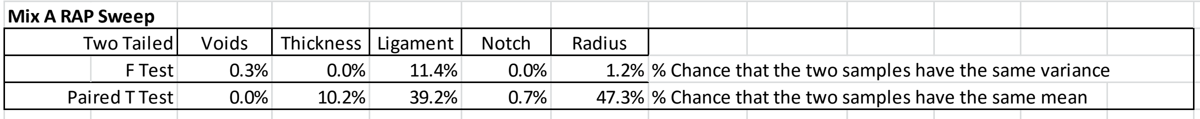

Mix A RAP Sweep

Two Tailed	Voids	Thickness	Ligament	Notch	Radius	
F Test	0.3%	0.0%	11.4%	0.0%	1.2%	% Chance that the two samples have the same variance
Paired T Test	0.0%	10.2%	39.2%	0.7%	47.3%	% Chance that the two samples have the same mean

The results of the paired t-test indicate that, for the RAP sweep, there is less than 50% chance that both labs are producing samples with the same geometries.

Table 5-5 Individual Technician Comparison, Mix B Binder Sweep

Mix B Binder Sweep						
CME	Average	Max	Min	Range	Std Dev	COV
Air Void Content	7.4	8	6.7	1.3	0.33	4.4%
Thickness	50.0	50.5	49.1	1.4	0.30	0.6%
Ligament	59.5	60.8	58.4	2.4	0.69	1.2%
Notch Depth	15.0	15.4	14.2	1.2	0.27	1.8%
Radius	74.5	75.8	73.5	2.3	0.64	0.9%
UDOT	Average	Max	Min	Range	Std Dev	COV
Air Void Content	6.4	7.3	5.5	1.8	0.56	8.7%
Thickness	50.0	50.5	49.6	0.9	0.26	0.5%
Ligament	59.4	60.6	58.4	2.2	0.68	1.1%
Notch Depth	15.1	15.4	14.7	0.7	0.20	1.3%
Radius	74.5	75.8	73.57	2.23	0.66	0.9%

Table 5-6 Individual Technician Comparison, Mix B RAP Sweep

Mix B RAP Sweep						
CME	Average	Max	Min	Range	Std Dev	COV
Air Void Content	7.8	8.8	6.8	2	0.61	7.8%
Thickness	50.2	50.6	49.7	0.9	0.26	0.5%
Ligament	60.0	61.4	58.1	3.3	0.78	1.3%
Notch Depth	14.7	16.3	13.9	2.4	0.48	3.3%
Radius	74.7	75.9	73.6	2.3	0.61	0.8%
UDOT	Average	Max	Min	Range	Std Dev	COV
Air Void Content	7.1	8.1	6.4	1.7	0.44	6.2%
Thickness	50.0	50.3	49.5	0.8	0.19	0.4%
Ligament	60.1	61.7	58.8	2.9	0.79	1.3%
Notch Depth	14.3	15.1	13.4	1.7	0.52	3.6%
Radius	74.4	75.4	73.4	2.0	0.60	0.8%

Based on the comparison presented in Table 5-5 and Table 5-6, the following observations are noted for each individual lab.

CME

- air voids: high with excessive scatter
- thickness: on target with excessive scatter for binder sweep
- ligament: on target with excessive scatter
- notch depth: on target with excessive scatter
- radius: slightly high with excessive scatter

UDOT

- air voids: low with excessive scatter for binder sweep
- thickness: on target with acceptable variation
- ligament: on target with excessive scatter
- notch depth: low with excessive scatter for RAP sweep
- radius: on target with excessive scatter

Table 5-7 Multi Lab Comparison, Mix B Binder Sweep

Mix B Binder Sweep						
Two Tailed	Voids	Thickness	Ligament	Notch	Radius	
F Test	0.2%	0.0%	96.1%	7.0%	86.1%	% Chance that the two samples have the same variance
Paired T Test	38.8%	0.0%	42.7%	4.6%	94.1%	% Chance that the two samples have the same mean

There results of the paired t-test for the binder sweep indicate that only the radius has a significant probability that both laboratories have the same values.

Table 5-8 Multi Lab Comparison, Mix B RAP Sweep

Mix B RAP Sweep						
Two Tailed	Voids	Thickness	Ligament	Notch	Radius	
F Test	5.9%	6.2%	91.9%	63.7%	95.1%	% Chance that the two samples have the same variance
Paired T Test	0.0%	0.1%	43.2%	0.2%	0.8%	% Chance that the two samples have the same mean

The results of the paired t-test for the RAP sweep indicate that there is very little chance that both labs are producing samples with similar geometries.

5.4 Conclusion on Variability of Results

All fracture tests exhibit a degree of variability greater than tests targeting properties developed prior to rupture. This particular test's geometry seems to have a particularly high degree of effect on the test results. It seems that the geometry of the test lends particular importance to sample thickness, notch thickness, and notch depth. Radius and thereby ligament length may play a minor role in the tail of the stress strain curve but this area of the curve is significantly confounded by the compression stress field. It has a minor effect on the integral and no effect on the slope at inflection. This leads to the deduction that the fabrication issues of highest importance are thickness, notch width and notch depth. It appears that density between 7 and 9 percent produce similar results while density below 7 percent generates much lower FI while also increasing variability.

None of the variables mentioned were well controlled by either technician nor were they well controlled between labs. Since the work was done on the same equipment by two trained technicians, it is evident that modifications to the tolerances are needed to reduce variability. The best repeatability and reproducibility were accomplished on the thickness cuts.

There is a consistent bias in the test results between the two labs. CME produces consistently higher test results than UDOT. Based on the data collected, it is unknown why this bias is present due to the randomness of the variability of the five metrics evaluated.

6.0 CONCLUSIONS

6.1 Summary

Adoption of any mixture test that relates to pavement performance requires an understanding of all aspects of mixture design. Factors such as binder content and addition of RAP are known to play a key role in the durability of pavements. The effects of two tests, the BBR and the IFIT, that target the low and intermediate properties of asphalt mixtures, respectively, were evaluated as part of this research work. The goal was not only to understand the capability of each tests to relate to performance but also to evaluate what effect they will have on asphalt mixtures produced in the state.

Specifically, this work aimed at answering the following questions:

1. How the introduction of low and intermediate temperature tests will affect the mixtures currently being used by UDOT in terms of binder content, RAP content, and aging?
2. What are potential changes in mixture design resulting from the incorporation of low and intermediate temperature tests?
3. Can mixture parameters (binder content, RAP content) be optimized using low temperature tests (BBR) and intermediate temperature test (IFIT)?
4. What is the repeatability of the IFIT tests and the ability of both BBR and SCB IFIT to detect changes in mixture components?

The experiment was separated into changes in binder content and air voids and RAP content and aging. The findings of these experiments are summarized next.

6.2 Findings

6.2.1 Binder Content and Air Voids

6.2.1.1 BBR

- For constant binder content, the higher the air voids the lower the modulus with no change in m-value
- Changes in binder content above optimum results in no significant changes in modulus or m-value. Changes in binder content below optimum results in the reduction of the modulus but no change in m-value.

6.2.1.2 IFIT

- As the binder content increases, the FI increases.
- The effect of air voids on FI is not clear as the experiment did not specifically target a wide range of air voids.

6.2.1.3 Overall Summary

While the FI seems to be a more sensitive parameter than the creep modulus or m-value to changes in binder content; the reverse is true for air voids. A decrease in creep modulus was observed with increased air voids but only a step function was seen in the FI.

While both tests show variations in results with changes in volumetrics (binder content and air voids), neither of these tests is expected to be used for volumetric verification as there are better tools available for this purpose.

6.2.2 RAP Content and Aging

6.2.2.1 BBR

- Both modulus and m-value are sensitive to changes in laboratory aging.
- Aging of the loose mixture at 135 ºC prior to compaction shows a more consistent trend that aging the compacted specimen at 80 ºC. Using the index valued developed in this study; equivalent times can be obtained between both conditioning procedures. One hour

of loose mix aging at 135 ºC results in the same mechanical changes as 47 to 55 hours of compacted mix aging at 80 ºC.

- The magnitude of the change in modulus and m-value resulting from aging is mixture dependent but is seems that for mixes with higher modulus, the rate of change is lower.
- Both modulus and m-value are sensitive to the additions of RAP. Even small quantities, like 15%, result in an increase in modulus and a decrease in m-value.

6.2.2.2 IFIT

- Aging reduces the FI, with lower decrease seen at high binder contents.
- As the RAP content increases, the FI decreases at a decreasing rate.
- At FI values below 10, the test seems to lose sensitivity.

6.2.2.3 Overall Summary

Both tests indicate that RAP is detrimental to the overall expected performance of the mixtures when compared to virgin mix. However, the data from the IFIT test indicates an asymptote as age increases and as RAP content increases while the data from the BBR shows no such trend. Based on this observations, the BBR appears to be a more sensitive test to capture the effect of aging and RAP on the material.

6.2.3 Variability of SCB IFIT

The geometry of the SCB test seems to have a particularly high degree of effect on the FI results. While the geometry of the test lends particular importance to sample thickness notch thickness and notch depth; radius and thereby ligament length may play a minor role in the tail of the stress strain curve.

The geometric variables mentioned were not well controlled by either technician nor were they well controlled between labs. Since the work was done on the same equipment by two trained technicians, it is evident that modifications to the equipment tolerances are needed to reduce variability.

There is a consistent bias in the test results between the two labs. CME produces consistently higher test results than UDOT. It is unknown why this bias is present due to the randomness of the variability of the five metrics evaluated.

6.3 Conclusions

Based on the work presented, the following conclusions are reached:

1. The results from the low and intermediate temperature tests (the BBR and the IFIT) indicate that increases in binder content are beneficial to the overall performance of the mixture (at least at low and intermediate temperatures). Deficiencies in binder content seem to be a problem for the BBR results as they indicate a desirable condition (lower modulus, same m-value), which is contrary to accepted knowledge. **Adoption of the IFIT would likely result in mixtures with higher binder content being favored during design; no such changes would be expected with the adoption of the BBR**.

2. The data from IFIT and BBR indicate aging causes mechanical changes in the material that relate to lower performance. The tests also indicate that RAP is detrimental to the overall expected performance of the mixtures when compared to virgin mixes. However, the data from the IFIT test indicates an asymptote as age increases and as RAP content increases while the data from the BBR shows no such limitation. Based on this observations, the BBR appears to be a more sensitive test to capture the effect of aging and RAP on the material. **Adoption of the BBR would likely result in changing the mixture design process to favor mixes with higher binder content with high RAP replacement.** Due to the limitations observed in the IFIT tests, such trend is difficult to assess at this time.

3. Conditioning the loose mixture at 135 ºC prior to compaction seems to be a practical method to accelerate the effect of aging when compared to conditioning the compacted specimen at 80 ºC. Even though 135 ºC could change the chemical composition of the binder, from the mechanical response, an equivalency can be established between field aging and laboratory aging that balances rigor and practicality**. Knowing the relationship between the different mixture parameters and the changes induced by aging gives the ability to optimize parameters such as binder and RAP content using the BBR and the IFIT.**

4. The variability and reproducibility of the IFIT needs to be further investigated before the test can be used with any degree of confidence.

6.4 Limitations and Challenges

The results from this work are limited to the conditions and materials that were used during this research. As was mentioned in Section 2.4, the IFIT and the BBR are at very different stages of development. Sample preparation, specimen conditioning, and testing variability is well understood for the BBR and as, such, **the BBR test is ready for implementation**. The IFIT, on the other hand, still presents many challenges regarding its reproducibility. Sample fabrication seems to be an issue that must be addressed before any attempt at adopting this test. Furthermore, questions still exist regarding the applicability of tests conditions such as temperature and rate of loading for local conditions.

As more data becomes available, some of the limitations can be better understood.

7.0 RECOMMENDATIONS AND IMPLEMENTATION

7.1 Recommendations

It is recommended that the BBR modulus and m-value be used as parameters to evaluate low temperature properties of asphalt mixtures. Using these parameters, a true performance-based specification can be developed at the mix design stage. The amount or condition of the test can be determined in an incremental manner. For example, if the proposed mixture results in low modulus and high m-value, then no further testing would be required. If the proposed mixture results in high modulus and low m-value then it would be rejected and must be redesigned. Finally, if the modulus and m-value fall within a transition zone, 3 hours of loose mixture aging at 135 ºC would be required prior to compaction. If after the aging conditioning the proposed mixture is still below the allowed modulus and above the minimum m-value, then the mixture would be acceptable; otherwise, it must be redesigned. As an example, data for a low design temperature of -22 ºC is shown in Figure 7-1 based on previous published work (Report No. UT-16.09).

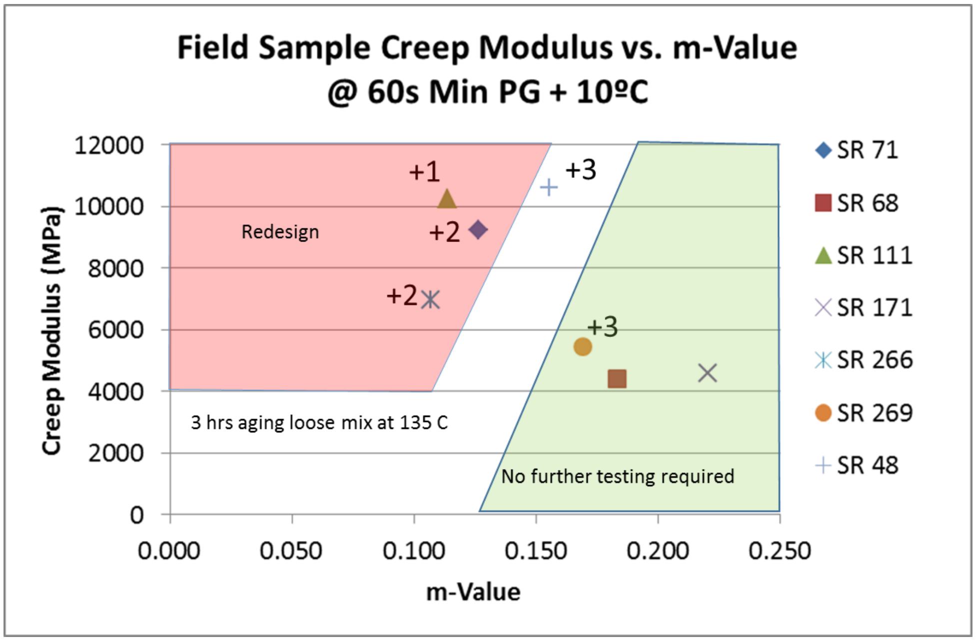

Figure 7-1 Proposed modulus and m-value limits at -12 ºC for mixtures prepared for a PG64-22 binder environment

The number next to the markers represent how many years since construction for cracks to appear.

Figure 7-1 shows three areas based on field performance: 1) accept with no further testing required, 2) redesign (i.e., reject), and 3) age the loose mix for 3 hours at 135 ºC then compact and test in the BBR. Unfortunately, limits for other temperature regions cannot be determined as part of this work since field data with results at the design temperature of -28 ºC are not available. Therefore, it is recommended that testing of field materials at -18 ºC be performed.

It is also recommended that further evaluation of the IFIT test be done to determine appropriate ranges for sample preparation parameters to reduce variability. The evaluation should be done using a third lab so that the multi-laboratory variability be understood. Once the variability and reproducibility are within reasonable ranges, studies should be done to determine the appropriate test temperature and loading rate.

7.2 Implementation Plan

Based on the information presented in this work, it is recommended that UDOT start implementing the BBR as a mixture test to evaluate the low temperature performance of asphalt pavements. Two simultaneous steps are recommended:

1. During the next paving seasons, asphalt mixtures should be collected from projects across the state. The mixtures should be tested and the pavement performance should be monitored. Using this updated information, a failure envelope similar to the one shown Figure 7-1 should be developed and eventually used as a performance based specification.

2. BBR equipment should be made available to regional labs so that staff can be properly trained in performing this test. This includes both samples preparation (i.e., cutting beams) and testing.

REFERENCES

AASHTO TP 105-13: *Standard Method of Test for Determining the Fracture Energy of Asphalt Mixtures Using the Semicircular Bend Geometry (SCB)*, American Association of State and Highway Transportation Officials, 2013.

AASHTO TP 124-16: *Provisional Standard Method of Test for Determining the Fracture Potential of Asphalt Mixtures Using Semicircular Bend Geometry (SCB) at Intermediate Temperature,* American Association of State and Highway Transportation Officials, 2016.

AASHTO R-30: *Standard Practice for Mixture Conditioning of Hot Mix Asphalt (HMA),* American Association of State and Highway Transportation Officials, 2016.

AASHTO T 166: *Standard Method of Test for Bulk Specific Gravity (Gmb) of Compacted Hot Mix Asphalt (HMA) Using Saturated Surface Dry Specimens,* American Association of State and Highway Transportation Officials, 2016.

AASHTO T 209: *Standard Method of Test for Theoretical Maximum Specific Gravity (Gmm) and Density of Hot Mix Asphalt (HMA),* American Association of State and Highway Transportation Officials, 2016.

Al-Qadi, I. L., Ozer, H., Lambros, J., El Khatib, A., Singhvi, P., Khan, T., ... and Doll, B.: *Testing protocols to ensure performance of high asphalt binder replacement mixes using RAP and RAS*. Illinois Center for Transportation/Illinois Department of Transportation, 2015

Al-Qadi, I, et al. (2016) "*Development of the fracture-based flexibility index for asphalt concrete cracking potential using modified semi-circle bending test parameters*" Journal of Building and Construction Materials, pp. 390-401. 2016

Arabani, M., and Ferdowsi, B. "*Evaluating the Semi-Circular Bending Test for HMA Mixtures."* International Journal of Engineering A: Basics, 22(1), Pp. 47-58. 2009

ASTM D8044-16: *Standard Test Method for Evaluation of Asphalt Mixture Cracking Resistance using the Semi-Circular Bend Test (SCB) at Intermediate Temperatures*, ASTM International, West Conshohocken, PA, 2016.

Bahia, H.U. and Anderson, D.A.: "*The Development of the Bending Beam Rheometer: Basic and Critical Evaluation of the Rheometer.*" Physical Properties of Asphalt Cement Binders, American Society of Testing and Materials, STP 1241, 28-50. 1995.

Clendennen, C., and Romero, P.: "*Evaluating the Representative Volume Element of Asphalt Concrete Mixture Beams for Testing in the Bending Beam Rheometer*." Multi-Scale Modeling and Characterization of Infrastructure Materials, N. Kringos, B. Birgisson, D. Frost, and L. Wang, Eds. Stockholm, Sweden ISBN 978-94-007-6877-2. Pp. 13-30. June, 2013.

EN 12697-44:2010: Bituminous Mixtures—Test Methods for Hot Mix Asphalt Part 44: Crack Propagation by Semi-Circular Bending Test, European Committee for Standardization, Brussels, Belgium, 2010.

Hajj, E. Y., P. E. Sebaalay, and D. Weitzel. "*Fatigue Characteristics of Superpave and Hveem Mixtures.*" Journal of Transportation Engineering, ASCE, Volume 131, Issue 4 pp. 302-10. 2005

Ho, C.H. and Romero, P: "*Using Asphalt Mixture Beams in the Bending Beam Rheometer*." International Journal of Road Materials and Pavement Design, Lavoisier ISSN 1468-0629, Volume 12 – No2/2011, Pp 293-314. 2011

Ho, C.H.: Control of Thermal-Induced Failures in Asphalt Pavements. Ph.D. Dissertation, University of Utah, Salt Lake City, Utah, 2010.

Ho, C.H. and Romero, P: "*Using Asphalt Mixture Beams in the Bending Beam Rheometer*." International Journal of Road Materials and Pavement Design, Lavoisier ISSN 1468-0629, Volume 12 – No2/2011, Pp 293-314. 2011

Hofman, R., Oosterbaan, B., Erkens, S. M. J. G., and van der Kooij, J.: "*Semi-circular* *bending test to assess the resistance against crack growth*". In 6th RILEM Symposium on performance testing and evaluation of bituminous materials, 2003, p 257-263.

Huang, B., Shu, X., and Zuo, G.: "*Using notched semi circular bending fatigue test to characterize fracture resistance of asphalt mixtures*." Engineering Fracture Mechanics, 109, 2013, p 78-88.

Huang, B., Shu, X., and Zuo, G.: "*Laboratory evaluation of semi-circular bending tensile strength test for HMA mixtures*." Transportation Research Board Annual Meeting, 2005.

Huang, L., Cao, K., and Zeng, M.: "*Evaluation of semicircular bending test for determining tensile strength and stiffness modulus of asphalt mixtures*." Journal of Testing and Evaluation, 37(2), 2009, p 1-7.

Jahanbakhsh, H., Karimi, M. M., and Tabatabaee, N.: *Experimental and numerical investigation of low-temperature performance of modified asphalt binders and mixtures*." Road Materials and Pavement Design, 2016, 1-22.

Jones, Z. Romero,P., and VanFrank, K.: "*Development of Low-Temperature Performance Specifications for Asphalt Mixtures using the Bending Beam Rheometer*." Journal of Road Materials and Pavement Design, Taylor Francis Volume 15, Issue 3, Pp 574-587. July 2014.

Krans, R. L., Tolman, F., and Van de Ven, M. F. C.: "*Semi-circular bending test: a practical crack growth test using asphalt concrete cores*." In RILEM proceedings, Chapman and Hall. 1996, p 123-132.

Mangiafico, S., Sauzeat, C., Di Benedetto, H., Pouget, S., Olard, F., and Planque, L.:" *Prediction of LVE Behavior of Mixtures Containing RAP from Properties of Base Constituents*." Transportation Research Procedia, Volume 14 Pp. 3552-3561, 2016.

Marasteanu, M., Velasquez, R., A. Cannone Falchetto, and Zofka, A. "*Development of a Simple Test to Determine the Low Temperature Creep Compliance of Asphalt Mixtures*." Final Report NCHRP Idea 133, 2009

Marasteanu M. O., Moon K. H., Zegeye Teshale E., Cannone Falchetto A., Turos M, Buttlar W., Braham A., Behnia B., Dave E., Paulino, Ahmed S., Leon S., Bahia H., Arshadi A., Tabatabaee H., Ojo J., Velasquez R., Mangiafico S., Williams C., Buss A., Bausano J., Kvasnak A., Gallistel A., McGraw J., "*Investigation of Low Temperature Cracking in Asphalt Pavements, Phase II*." National Pooled Fund Study – Phase II, Final Report, Minnesota Department of Transportation, 2012.

Marasteanu, M., Zofka, A., Turos, M., Li, X., Velasquez, R., Li, X., and Ojo, J. Investigation of low temperature cracking in asphalt pavements. National pooled Fund Study 776, 2007.

Marasteanu, M.: "*The Role of Bending Beam Rheometer Parameters in Thermal Stress Calculations*." Transportation Research Record No. 1875, pp. 9-13. 2004.

Molenaar, A. A. A., Scarpas, A., Liu, X., and Erkens, S. M. J. G.: "*Semi-circular bending test; simple but useful?.* Journal of the Association of Asphalt Paving Technologists, Volume 71, Pp 794-815. 2002.

Mohammad, L. N., Wu, Z., and Aglan, M. A. "*Characterization of fracture and fatigue resistance on recycled polymer-modified asphalt pavements*." In Proceedings of the RILEM: 5th International Conference on Cracking in Pavements Mitigation, Risk Assessment and Prevention, France, 2004, p 375-382.

Mohammad, L. N., Kim, M., and Elseifi, M. "*Characterization of asphalt mixture's fracture resistance using the semi-circular bending (SCB) test*". 7th RILEM international conference on cracking in pavements, Springer Netherlands. 2012, p 1-10.

Mull, M. A., Stuart, K., and Yehia, A.: "*Fracture resistance characterization of chemically modified crumb rubber asphalt pavement*." Journal of Materials Science, 37(3), 2002, 557-566.

Mull-Aglan, M. A., and Othman, A. Mohammad, L. N., "*Fatigue crack growth analysis of hot-mix asphalt employing semicircular notched bend specimen*. " Transportation research board 85th annual meeting (No. 06-1665), 2006.

Nsengiyumva, G., Kim, Y. R., and You T.: *Development of a Semicircular Bend (SCB) Test Method for Performance Testing of Nebraska Asphalt Mixtures*. Report 12-2015, Nebraska LTAP, 2015.

Romero, P., *Using the Bending Beam Rheometer for Low Temperature Testing of Asphalt Mixtures*. Report No. UT-16.09. Utah Department of Transportation. Salt Lake City, UT, July 2016.

Romero, P., Ho, C.H., and VanFrank, K.: *Development of Methods to Control Cold Temperature and Fatigue Cracking for Asphalt Mixtures*. Report No. UT-10-08. Utah Department of Transportation, Salt Lake City, UT. May 2011.

Underwood, S., Baek, C., and Kim, Y.R.: "*Simplified Viscoelastic Continuum Damage Model as Platform for Asphalt Concrete Fatigue Analysi"s*. Transportation Research Record: Journal of the Transportation Research Board, No. 2296, Transportation Research Board of the National Academies, Washington, D.C., 2012, pp. 36–45.

VanFrank, K., VanMilligen, M., and Biel, T.: *Intermediate Temperature Cracking in HMA, Phase I: Semi-Circular Bending (SCB) Practicality Evaluation*. Report No. UT-17.01. Utah Department of Transportation, Salt Lake City, UT 2017

Wang, H., Zhang, C., Li, L., You, Z., and Diab, A. "*Characterization of Low Temperature Crack Resistance of Crumb Rubber Modified Asphalt Mixtures Using Semi-Circular Bending Tests*." Journal of Testing and Evaluation, 44(2), 2016, p 847-855.

Zofka, A., and Braham, A. “*Comparison of low-temperature field performance and laboratory testing of 10 test sections in the Midwestern United States”*. Transportation Research Record: Journal of the Transportation Research Board, (2127), 2009, 107-114.

Zofka, A., Marasteanu, M. O., Li, Xinjun, Clyne, T. R., McGraw, J. *Simple Method to Obtain Asphalt Binders Low Temperature Properties from Asphalt Mixtures Properties*. In the Journal of the Association of Asphalt Paving Technologists, 2005, Vol. 74, pp. 255-282.

APPENDIX A: IFIT Sample Preparation Protocol

SCB Binder Sweep Test Protocol IFIT Method

The method used to prepare the samples for IFIT binder sweep testing is as follows:

Binder content: Target ± 0.5 Percent of total mix

Two Mix Designs

Test consists of four samples

Three replicates

Number of Samples per mix design = 36

Four samples per puck. Determine where to cut the puck to balance voids.

Puck Height 160 mm

Number of Pucks per mix design = 9

Target void on full puck 7.0 ± 0.5% Use Calculated Rice

Mixing temp 320F

Compaction temp 305F

Short Term Aging 2 hours

Mix A: 19.5mm 100 gyration 4.6% Target Binder 4.1, 4.6, 5.1

Mix B: 12.5 mm 75 Gyration 5.25% Target Binder 4.75, 5.25, 5.75

Binder: Calumet 64-28 2014

Compact to height and weight to produce target void

Mix A, Gmm = 2.511 at 4.6% Binder

Mix V, Gmm = 2.402 at 5.25% Binder

Use the TestQuip machine and analysis software

Measure sample width, Height and Chord length. Notch depth = H-C

Test Temp 25±0.5C

Determine Gsb on cut and uncut sample on puck #4 and up.

Compact first day, cut and break on next day

Use Testquip jigs for cutting.

Use a dummy puck for temperature conditioning. Subject dummy puck to all conditions related to sample prep including soaking in blade cooling water.

APPENDIX B: DATA

BBR Results and Data Management

All of the data from BBR testing was collected using electronic data acquisition of force, displacement, and temperature sensors. The data was collected in non-proprietary CSV format as generated by the BBR data acquisition system. Spreadsheets were used to summarize and analyzed the data. The raw data, called primary data, has been preserved and archived at Zenodo (https://zenodo.org/), an international repository/archive of research outputs from across all fields of research. Zenodo is listed as conforming with the USDOT Public Access Plan (https://ntl.bts.gov/publicaccess/repositories.html). According to Zenodo's policy, data entries remain accessible forever.

The data is accessible at the following link: http://doi.org/10.5281/zenodo.1035944

Romero, Pedro. (2017). Balanced Asphalt Concrete Mix Performance Phase II: Analysis of BBR Tests [Data set]. Zenodo.

A README file, including the metadata/information required to repeat the research, is included along with the data in the archive. Zenodo will provide proper citation for users to incorporate the data into their publications and will have a memorandum of understanding (MOU) stating that users may not re-release the data to a third party, but direct them back to the repository.

Summarized data, called secondary data, is presented in the following tables the mixture ID refers to the mixture used (Mix A or Mix B) follow by RXX (RAP content, in percent), L for loose mixture and C for compacted mixture and then either the hours at 135 ºC (for loose mix) or the days at 80 ºC (for compacted mix). Fox example, AR15C5d stands for Mixture A with 15 percent RAP aged in the compacted state for 5 days.

Table 0-1 BBR Results for Mixture A

Bending Beam Rheometer Test Results of Mixture A specimens							
Mixture ID	**Samples Tested**	**Trimmed Stiffness, Mpa (Omitting Max and Min)**			**Trimmed m-value (Omitting Max and Min)**		
		Average	**Standard Deviation**	**CoV (%)**	**Average**	**Standard Deviation**	**CoV (%)**
CAR0	24	15418	1256	8.15	0.131	0.010	7.56
AR0L3h	18	15900	2076	13.06	0.124	0.014	11.66
AR0L6h	18	16581	1687	10.17	0.126	0.014	11.08
CAR15	18	17606	1555	8.83	0.116	0.009	7.58
AR15L3h	19	17265	2365	13.70	0.106	0.014	13.29
AR15L6h	18	18175	2176	11.97	0.110	0.011	10.10
CAR25	18	18813	2655	14.12	0.108	0.010	9.47
AR25L3h	18	17061	1976	11.58	0.090	0.009	9.98
AR25L6h	17	18373	1636	8.90	0.119	0.021	17.71
CAR35	19	18844	1470	7.80	0.096	0.010	9.98
AR35L3h	18	18644	1765	9.46	0.097	0.010	10.82
AR35L6h	17	18988	2104	11.08	0.088	0.010	11.00
AR0C2d	18	13775	2102	15.26	0.150	0.011	7.15
AR0C5d	20	15306	1880	12.28	0.134	0.012	9.18
AR0C7d	17	15793	1390	8.80	0.123	0.014	11.36
AR15C2d	17	17007	1623	9.55	0.106	0.009	8.22
AR15C5d	18	18531	1657	8.94	0.131	0.013	10.17
AR15C7d	18	15563	1453	9.34	0.107	0.011	10.69
AR25C2d	15	18877	2547	13.49	0.101	0.005	5.31
AR25C5d	18	17794	2235	12.56	0.107	0.011	10.45
AR25C7d	19	17372	1279	7.36	0.093	0.009	9.89
AR35C2d	18	19467	2895	14.87	0.106	0.010	9.17
AR35C5d	17	19360	2647	13.67	0.100	0.010	10.16
AR35C7d	18	21680	2465	11.37	0.096	0.014	14.30

Table 0-2 BBR Results for Mixture B

Bending Beam Rheometer Test Results for Mixture B specimens							
Mix ID	**Samples Tested**	**Trimmed Stiffness, MPa (Omitting Max and Min)**			**Trimmed m-value (Omitting Max and Min)**		
		Average	**Standard Deviation**	**CoV (%)**	**Average**	**Standard Deviation**	**CoV (%)**
CBR0	24	12504	1241	9.92	0.154	0.013	8.29
CBR15	17	13747	1200	8.73	0.136	0.012	8.42
CBR25	18	14863	1221	8.22	0.123	0.011	9.27
CBR35	18	16963	1610	9.49	0.108	0.011	9.96
BR0L3h	18	12944	1186	9.17	0.146	0.011	7.28
BR15L3h	18	14206	2148	15.12	0.124	0.009	7.44
BR25L3h	17	15680	1182	7.54	0.118	0.012	9.99
BR35L3h	18	17338	1953	11.26	0.106	0.007	6.50
BR0L6h	17	14038	1965	14.00	0.134	0.015	11.33
BR15L6h	18	16644	2219	13.33	0.123	0.006	4.84
BR25L6h	16	17186	2169	12.62	0.112	0.013	11.63
BR35L6h	16	18400	2048	11.13	0.104	0.008	7.40
BR0C2d	18	12863	933	7.25	0.151	0.009	5.58
BR15C2d	18	14400	1345	9.34	0.133	0.012	9.20
BR25C2d	18	15900	1664	10.46	0.120	0.010	8.77
BR35C2d	18	17056	1705	10.00	0.104	0.008	7.70
BR0C5d	18	13694	1274	9.31	0.147	0.009	6.15
BR15C5d	18	14581	1492	10.23	0.119	0.010	8.45
BR25C5d	18	15969	1464	9.17	0.115	0.009	7.78
BR35C5d	18	17136	1185	6.92	0.105	0.010	9.55
BR0C7d	17	13800	1500	10.87	0.134	0.012	8.90
BR15C7d	17	15160	1579	10.41	0.125	0.013	10.46
BR25C7d	17	17107	2071	12.11	0.117	0.012	10.58
BR35C7d	17	17987	1817	10.10	0.109	0.016	14.92

IFIT Results (on next page)

Mix A Binder Sweep

	CME	CME	CME	CME	CME	CME	CME	CME	CME	CME	CME	CME	CME	CME	CME	CME	CME	CME	CME	CME	CME	CME	CME	CME	CME	CME	CME	CME	CME	CME	CME	CME	CME	CME	CME	CME
Specimen ID	D41T1	D41T2	D41B1	D41B2	E41T1	E41T2	E41B1	E41B2	F41T1	F41T2	F41B1	F41B2	E46BB	E46TA	E46TB	E46BA	G46TA	G46BA	G46TB	G46BB	F46BA	F46BB	F46TB	F46TA	D51T1	D51T2	D51B1	D51B2	E51T1	E51T2	E51B1	E51B2	F51T1	F51T2	F51B1	F51B2
Air Void Content	6.4	6.4	5.9	5.9	6.7	6.7	6.2	6.2	6.4	6.4	6.6	6.6	6.5	6.5	6.7	6.7	6.2	5.5	5.5	5.7	5.7	6.1	6.1	6.2	6.6	6.6	6.0	6.0	6.3	6.3	6.1	6.1	5.6	5.6	6.6	6.6
Thickness	49.9	49.9	49.8	50.0	50.2	49.9	49.9	49.7	49.4	50.0	49.8	49.9	49.9	50.5	50.0	50.5	49.6	50.2	50.1	49.9	49.9	50.1	49.9	50.2	49.8	49.4	49.5	49.3	49.1	49.7	50.1	50.2	50.2	50.2	49.8	50.1
Ligament	58.9	59.6	59.8	58.6	59.9	59.1	59.2	58.7	59.7	59.1	59.7	59.2	58.9	60.0	60.5	58.9	58.9	58.5	60.2	58.4	59.9	59.6	58.6	59.2	60.1	59.5	59.5	59.6	60.3	59.2	60.0	59.0	59.9	59.6	60.0	59.2
Notch Depth	15.3	15.3	15.2	15.2	15.0	14.8	15.3	15.2	15.2	14.9	15.1	15.0	15.3	15.1	15.3	15.1	15.3	15.1	15.2	15.4	15.1	15.3	15.3	15.4	14.5	14.9	14.8	14.8	14.7	15.1	14.7	14.9	14.5	14.6	14.7	15.1
Radius	74.2	74.9	75.0	73.8	74.9	73.9	74.5	73.9	74.9	74.0	74.8	74.2	74.2	75.1	75.8	74.0	74.2	73.6	75.4	73.8	75.0	74.9	73.9	74.6	74.6	74.4	74.3	74.4	75.0	74.3	74.7	73.9	74.4	74.2	74.7	74.3

	UDOT	UDOT	UDOT	UDOT	UDOT	UDOT	UDOT	UDOT	UDOT	UDOT	UDOT	UDOT													UDOT	UDOT	UDOT	UDOT	UDOT	UDOT	UDOT	UDOT		UDOT		
Specimen ID	41 A	82 A	123	164	205 A	246 A	287	328	369 A	410 A	451	492	4.60 A	9.20 A	13.80	18.40	23.00	27.60	32.20	36.80	41.40	46.00	50.60	55.20	51 A	102 A	153	204	255 A	306 A	357	408	Sample 9	Sample 10	Sample 11	Sample 12
Air Void Content	7.1	7.1	7.3	7.3	7.5	7.5	6.0	6.0	7.6	7.5	7.7	7.7	6.5	6.5	6.7	6.7	6.2	6.2	5.5	5.5	5.7	5.7	6.1	6.1	7.2	7.2	7.3	7.3	7.5	7.5	7.2	7.2	7.7	7.7	6.8	6.8
Thickness	50.2	50.1	50.7	50.5	50.3	50.2	50.1	49.9	50.4	50.5	50.7	50.7	49.9	50.5	50.0	50.5	50.2	49.6	50.2	50.1	49.9	49.9	50.1	49.9	49.6	49.7	49.8	49.9	49.7	49.6	49.9	50.0	50.1	50.1	50.0	50.0
Ligament	59.7	58.9	59.9	60.0	59.4	59.4	59.8	59.3	60.3	59.1	60.4	59.0	58.9	60.0	60.5	58.9	59.2	58.9	58.5	60.2	58.4	59.9	59.6	58.6	60.3	59.2	60.0	59.4	60.0	59.8	60.1	59.9	60.1	59.3	60.5	59.2
Notch Depth	15.0	14.8	14.8	14.4	14.4	14.4	14.8	15.0	14.8	14.7	15.1	14.9	15.3	15.1	15.3	15.1	15.4	15.3	15.1	15.2	15.4	15.1	15.3	15.3	14.7	14.7	14.7	14.8	14.5	14.6	14.4	14.3	14.3	14.6	14.3	14.6
Radius	74.7	73.8	74.8	74.4	73.7	73.7	74.7	74.3	75.0	73.7	75.5	73.8	74.2	75.1	75.8	74.0	74.6	74.2	73.6	75.4	73.8	75.0	74.9	73.9	75.0	73.9	74.8	74.1	74.5	74.4	74.6	74.2	74.4	73.9	74.8	73.8

Mix A RAP Sweep

	CMETG	CMETG	CMETG	CMETG	CMETG	CMETG	CMETG	CMETG	CMETG	CMETG	CMETG	CMETG	CME	CME	CME	CME	CME	CME	CME	CME	CME	CME	CME	CME	CME	CME	CME	CME	CME	CME	CME	CME	CME	CME	CME	CME
Specimen ID	S15DB1	S15DB2	S15DT1	S15DT2	S15EB1	S15EB2	S15ET1	S15ET2	S15FB1	S15FB2	S15FT1	S15FT2	S25AB1	S25AB2	S25AT1	S25AT2	S25BB1	S25BB2	S25BT1	S25BT2	S25CB1	S25CB2	S25CT1	S25CT2	S35AB1	S35AB2	S35AT2	S35AT2	S35BB1	S35BB2	S35BT1	S35BT2	S35CB1	S35CB2	S35CT1	S35CT2
Air Void Content	7.10	7.10	7.20	7.20	7.10	7.10	7.40	7.40	6.60	6.60	7.30	7.30	5.90	5.90	6.30	6.30	5.00	5.00	6.00	6.00	6.00	6.00	6.00	6.00	5.60	5.60	6.30	6.30	6.00	6.40	6.00	6.00	6.20	6.20	6.40	6.40
Thickness	50.00	49.80	49.80	49.80	50.00	50.10	50.10	49.70	49.60	49.50	49.80	61.50	50.00	50.30	49.60	49.70	49.80	49.80	49.60	49.50	49.90	49.80	59.80	49.90	49.90	50.10	49.70	49.70	49.80	49.50	49.90	50.40	49.70	49.90	49.90	49.80
Ligament	59.50	60.70	60.60	59.30	59.30	60.90	59.60	61.40	61.30	59.30	59.00	59.80	59.60	60.30	59.40	60.70	59.50	60.10	59.50	60.60	59.60	60.40	60.30	59.60	59.50	60.60	60.10	60.10	59.40	60.40	59.60	60.90	60.50	60.40	60.00	60.30
Notch Depth	14.30	13.90	14.10	14.00	14.40	14.50	13.80	14.10	14.30	14.60	16.20	14.40	14.80	14.60	14.60	14.80	14.60	14.90	14.80	14.40	14.60	14.40	14.70	14.70	14.30	14.30	14.30	14.30	14.40	14.40	13.90	14.50	14.80	14.00	14.20	14.50
Radius	73.80	74.60	74.70	73.30	73.70	75.40	73.40	75.50	75.60	73.90	75.20	74.20	74.43	74.85	74.00	75.55	74.11	75.00	74.32	75.00	74.17	74.78	75.07	74.27	73.84	74.92	74.39	74.39	73.86	74.87	73.48	75.34	75.26	74.32	74.13	74.75

	UDOT	UDOT	UDOT	UDOT	UDOT	UDOT	UDOT	UDOT	UDOT	UDOT	UDOT	UDOT	UDOT	UDOT	UDOT	UDOT	UDOT	UDOT	UDOT	UDOT	UDOT	UDOT	UDOT	UDOT	UDOT	UDOT	UDOT	UDOT	UDOT	UDOT	UDOT	UDOT	UDOT	UDOT	UDOT	UDOT
Specimen ID	15	30	45	60	75	90	105	120	135	150	165	180	25	50	75	100	125	150	175	200	225	250	275	300	35	70	105	140	175	210	245	280	315	350	385	420
Air Void Content	6.9	6.9	6.9	6.9	7.5	7.5	7.2	7.2	7.4	7.4	7.3	7.3	6.6	6.6	7.7	7.7	7.4	7.4	7.7	7.7	7.6	7.6	7.5	7.5	7.8	7.8	7.5	7.5	7.8	7.8	8.0	8.0	7.8	7.8	8.0	8.0
Thickness	49.9	49.6	49.5	49.9	49.1	49.3	49.7	49.5	49.7	50.0	49.7	49.3	49.6	49.2	50.0	49.6	50.0	49.9	49.8	49.8	49.9	49.5	49.7	49.4	50.2	49.7	49.6	49.8	50.0	49.6	49.7	49.5	49.9	50.2	50.0	49.7
Ligament	59.9	60.1	59.6	60.5	59.9	60.2	60.0	60.5	59.6	60.6	59.9	60.6	60.4	60.0	60.7	60.8	60.3	60.1	60.9	60.9	60.6	60.0	60.3	59.6	59.4	59.9	60.2	59.7	60.6	59.9	61.1	59.2	60.8	59.8	60.3	59.6
Notch Depth	14.2	14.4	14.4	14.2	14.4	14.3	14.3	14.1	14.4	14.2	14.3	14.0	14.1	14.1	14.0	14.1	14.3	14.2	13.9	14.0	14.1	14.0	14.3	14.5	14.9	14.3	14.5	14.4	14.2	14.1	14.2	14.2	14.3	13.9	14.4	14.1
Radius	74.1	74.5	74.0	74.7	74.3	74.5	74.3	74.5	74.0	74.8	74.2	74.6	74.5	74.1	74.8	74.8	74.6	74.2	74.8	74.9	74.8	74.0	74.6	74.1	74.4	74.2	74.8	74.1	74.8	74.0	75.3	73.5	75.1	73.6	74.7	73.8

Mix B Binder Sweep

	CME	CME	CME	CME	CME	CME	CME	CME	CME	CME	CME	CME	1	2	3	4	5	6	7	8	9	10	11	12	CME	CME	CME	CME	CME	CME	CME	CME	CME	CME	CME	
Specimen ID	A48T1	A48T2	A48B1	A48B2	B48T1	B48T2	B48B1	B48B2	C48T1	C48T2	C48B1	C48B2	A53T1	A53T2	A53B1	A53B2	B53T1	B53T2	B53B1	B53B2	C53T1	C53T2	C53B1	C53B2	A58T1	A58T2	A58B1	A58B2	B58T1	B58T2	B58B1	B58B2	C58T1	C58T2	C58B1	C58B2
Air Void Content	7.5	7.5	7.5	7.5	7.7	7.7	7.1	7.1	7.2	7.2	7.7	7.7	8.0	8.0	7.7	7.7	6.7	6.7	7.5	7.5	7.4	7.4	7.0	7.0	7.4	7.4	7.1	7.1	7.8	7.8	7.1	7.1	7.1	7.1	7.3	7.3
Thickness	50.0	50.1	50.0	49.4	50.1	50.2	50.0	50.2	50.2	49.8	50.0	49.8	50.0	50.5	49.9	50.5	50.2	50.1	50.2	49.6	50.1	49.9	49.9	49.9	50.3	50.3	49.3	50.1	50.0	50.3	50.2	49.9	50.4	50.0	50.3	49.1
Ligament	59.7	59.3	59.5	59.4	60.8	58.5	59.6	59.4	59.7	59.4	59.0	59.6	60.5	58.9	58.9	60.0	58.5	60.2	59.2	58.9	59.6	58.6	58.4	59.9	60.6	59.1	60.6	58.6	59.2	60.4	60.7	59.1	60.5	59.0	59.9	59.6
Notch Depth	14.9	15.0	15.0	15.1	14.7	15.0	14.8	14.9	14.8	14.7	15.2	15.2	15.3	15.1	15.3	15.1	15.1	15.2	15.4	15.3	15.3	15.3	15.4	15.1	14.7	14.9	15.1	15.0	14.7	15.0	14.2	14.9	15.0	14.5	14.6	14.8
Radius	74.6	74.3	74.5	74.5	75.5	73.5	74.4	74.3	74.5	74.1	74.2	74.8	75.8	74.0	74.2	75.1	73.6	75.4	74.6	74.2	74.9	73.9	73.8	75.0	75.3	74.0	75.7	73.6	73.9	75.4	74.9	74.0	75.5	73.5	74.5	74.4

	UDOT												UDOT	UDOT	UDOT	UDOT	UDOT	UDOT	UDOT	UDOT	UDOT	UDOT	UDOT	UDOT					UDOT							
Specimen ID	475 A	950 A	1425.0	1900.0	23.75	23.75	33.25	38.00	42.75	47.50	52.25	57.00	525 A	1050 A	1575	2100	2625 A	3150 A	3675	4200	4725 A	5250 A	5775	6300	575 A	1150 A	1725.0	2300.0	2875 A	3450 A	4025.0	4600.0	5175 A	5750 A	6325.0	6900.0
Air Void Content	6.5	6.5	6.7	6.7	6.2	6.2	5.5	5.5	5.7	5.7	6.1	6.1	7.1	7.1	6.8	6.8	7.3	7.3	6.7	6.7	7.1	7.1	7.0	7.0	6.5	6.5	6.7	6.7	6.2	6.2	5.5	5.5	5.7	5.7	6.1	6.1
Thickness	49.9	50.5	50.0	50.5	50.2	49.6	50.2	50.1	49.9	49.9	50.1	49.9	49.8	49.9	49.7	49.8	49.7	49.8	49.6	49.8	49.6	49.8	49.6	49.9	49.9	50.5	50.0	50.5	50.2	49.6	50.2	50.1	49.9	49.9	50.1	49.9
Ligament	58.9	60.0	60.5	58.9	59.2	58.9	58.5	60.2	58.4	59.9	59.6	58.6	59.7	59.3	60.2	58.6	59.7	59.0	60.1	58.9	60.2	59.0	60.6	59.0	58.9	60.0	60.5	58.9	59.2	58.9	58.5	60.2	58.4	59.9	59.6	58.6
Notch Depth	15.3	15.1	15.3	15.1	15.4	15.3	15.1	15.2	15.4	15.1	15.3	15.3	15.0	14.9	14.8	14.9	15.0	15.0	15.0	15.0	14.9	14.8	14.8	14.7	15.3	15.1	15.3	15.1	15.4	15.3	15.1	15.2	15.4	15.1	15.3	15.3
Radius	74.2	75.1	75.8	74.0	74.6	74.2	73.6	75.4	73.8	75.0	74.9	73.9	74.7	74.2	75.0	73.6	74.7	74.0	75.1	73.8	75.1	73.7	75.3	73.7	74.2	75.1	75.8	74.0	74.6	74.2	73.6	75.4	73.8	75.0	74.9	73.9

Mix B RAP Sweep

	CMETG	CMETG	CMETG	CMETG	CMETG	CMETG	CMETG	CMETG	CMETG	CMETG	CMETG	CMETG	CME	CME	CME	CME	CME	CME	CME	CME	CME	CME	CME	CME	CME	CME	CME	CME	CME	CME	CME	CME	CME	CME	CME	CME
Specimen ID	G15DB1	G15DB2	G15DjT1	G15DjT2	G15EB1	G15EB2	G15ET1	G15ET2	G15FB1	G15FB2	G15FT1	G15FT2	G25DB1	G25DB2	G25DT1	G25DT2	G25EB1	G25EB2	G25ET1	G25ET2	G25FB1	G25FB1	G25FT1	G25FT2	G35DB1	G35DB2	G35DT1	G35DT2	G35EB1	G35EB2	G35ET1	G35ET2	G35FB1	G25FB2	G35FT1	G35FT2
Air Void Content	7.3	7.3	7.6	7.6	6.8	6.8	7.2	7.2	7.1	7.1	6.8	6.8	7.9	7.9	8.1	8.1	7.2	7.2	7.7	7.7	7.7	7.7	8.8	8.8	8.1	8.1	8.7	8.7	8.2	8.2	8.5	8.5	8.2	8.2	8.2	8.2
Thickness	49.7	49.8	50.1	50.1	49.7	49.8	49.8	49.7	50	50	50.1	50.4	50.4	50.6	50.5	50.3	50.3	50.5	50.5	50.5	50.2	50.2	50	50.0	49.9	50.3	50.2	50.4	50.2	50.3	50.3	50.0	50.3	50.2	50.5	50.5
Ligament	60.7	59	59.8	60.5	60.2	59.7	59.7	60.4	59.1	60.4	59.4	60.1	60.7	59.8	59.5	59.5	59.5	58.1	60.1	59.1	61.1	61.1	61.0	61.0	61.0	59.4	59.9	59.1	61.4	59.2	59.9	58.8	59.8	59.4	60.7	60.7
Notch Depth	14.4	14.9	14.5	14.4	14.3	15.1	14.1	14.9	14.9	14.5	14.6	14.8	14.1	14.3	14.8	14.8	15.5	16.3	15.3	14.9	14.2	14.2	14.2	14.0	14.9	14.9	15.4	14.7	13.9	14.4	14.9	15.2	14.6	14.6	14.8	14.8
Radius	75.1	73.9	74.3	74.9	74.5	74.8	73.8	75.3	74.0	74.9	74.0	74.9	74.8	74.1	74.3	74.3	75.0	74.4	75.4	74.0	75.3	75.3	75.2	75.0	75.9	74.3	75.3	73.8	75.3	73.6	74.8	74.0	74.4	74.0	75.5	75.5

	UDOT	UDOT	UDOT	UDOT	UDOT	UDOT	UDOT	UDOT	UDOT	UDOT	UDOT	UDOT	UDOT	UDOT	UDOT	UDOT	UDOT	UDOT	UDOT	UDOT	UDOT	UDOT	UDOT	UDOT	UDOT	UDOT	UDOT	UDOT	UDOT	UDOT	UDOT	UDOT	UDOT	UDOT	UDOT	UDOT
Specimen ID	44	88	132	176	220	264	7B6	352	396	440	484	528	25	50	75	100	125	150	175	200	225	250	275	300	35	70	105	140	175	210	245	280	315	350	385	420
Air Void Content	7.4	7.4	7.2	7.2	7.7	7.7	7.6	7.6	8.1	8.1	7.5	7.5	6.8	6.8	6.6	6.6	7.1	7.1	7.0	7.0	7.0	7.0	6.9	6.9	6.6	6.6	6.4	6.4	6.9	6.9	6.8	6.8	7.2	7.2	6.6	6.6
Thickness	50.2	50.1	49.9	50.2	49.8	50.3	49.9	50.1	50.1	50.2	50.2	50.2	49.9	49.8	50.0	50.0	49.6	49.8	50.0	49.9	49.7	49.8	49.8	50	50.1	50.1	50.0	50.1	50.0	49.8	49.5	49.9	50.0	50.0	49.6	49.8
Ligament	59.9	58.8	59.8	58.8	60.0	59.0	59.9	59.0	60.0	58.9	59.8	59.3	59.8	60.2	60.4	59.7	61.0	59.9	61.4	59.5	60.5	60.0	61.0	60.0	60.9	59.5	61.0	60.0	61.7	59.9	61.5	59.9	61.5	59.7	61.1	60.0
Notch Depth	15	14.9	14.9	15.1	15.0	14.8	14.9	15.0	14.9	15.1	14.8	14.8	14.4	14.2	14.3	14.3	14.1	14.1	13.9	14.1	14.1	14.1	14.0	13.8	14.3	13.9	14.1	13.6	13.7	13.6	13.4	13.9	13.6	13.8	13.7	13.8
Radius	74.9	73.8	74.6	73.9	75.0	73.8	74.8	74.0	74.9	74.0	74.5	74.2	74.2	74.4	74.7	74.0	75.1	73.9	75.2	73.6	74.7	74.2	74.9	73.8	75.3	73.4	75.1	73.6	75.4	73.5	74.9	73.9	75.2	73.5	74.9	73.8